Influence of Dissolved Oxygen on the Composition and Stability of the Solid–Electrolyte Interphase on Lithium Electrodes.

Dem Fachbereich Biologie und Chemie
der Justus-Liebig-Universität Gießen
vorgelegte Dissertation zur Erlangung
des akademischen Grades
Doktor der Naturwissenschaften
– Dr. rer. nat. –

Ronja Haas

June 2023

Dekan:	Prof. Dr. Thomas Wilke
1. Gutachter:	Prof. Dr. Jürgen Janek
2. Gutachter:	Prof. Dr. Daniel Schröder
Eingereicht am	15. Juni 2023

Eidesstattliche Erklärung

Hiermit versichere ich, die vorgelegte Arbeit selbstständig und ohne unerlaubte fremde Hilfe und nur mit den Hilfen angefertigt zu haben, die ich in der Arbeit angegeben habe. Alle Textstellen, die wörtlich oder sinngemäß aus veröffentlichten Schriften entnommen sind, und alle Angaben, die auf mündlichen Auskünften beruhen, sind als solche kenntlich gemacht. Bei den von mir durchgeführten und in der Arbeit erwähnten Untersuchungen habe ich die Grundsätze guter wissenschaftlicher Praxis, wie sie in der „Satzung der Justus-Liebig-Universität zur Sicherung guter wissenschaftlicher Praxis" niedergelegt sind, eingehalten. Gemäß § 25 Abs. 6 der Allgemeinen Bestimmung für modularisierte Studiengänge dulde ich eine Überprüfung der Arbeit mittels Anti-Plagiatssoftware.

Gießen, 15.06.2023

Ronja Haas

Abstract

Aprotic Li–O_2 batteries are considered promising energy storage devices for mobile applications, as they have a high theoretical energy density that significantly exceeds that of state of the art lithium-ion batteries. However, they are still far from commercialization as they suffer from low lifetime and high charge overpotential. A further problem are numerous degradation reactions, many of which are related to dissolved O_2. This work investigates the influence of O_2 dissolved in the liquid electrolyte on the lithium anode, which could not be clarified in the literature so far.

First, a systematic study of the solubility and diffusion of O_2 in different electrolytes is performed. Both an experimental approach and molecular dynamics simulations are used to determine the diffusion coefficient. Good agreement is found between theory and experiment, demonstrating that both methods are suitable for the determination of the diffusion coefficient. Moreover, a correlation between the experimentally determined O_2 solubility and the surface tension of the solvent is established, which will allow the prediction of O_2 solubility in other solvents in the future. Overall, these findings significantly reduce the amount of work required to determine O_2 solubility and diffusivity, thus facilitating the transfer of the results to other electrolytes.

Since it was previously unclear, due to conflicting literature, whether dissolved O_2 has a positive or negative effect on the stability of the lithium metal anode, this issue is further investigated. Lithium deposition and dissolution experiments demonstrate that the Coulomb efficiency can be significantly increased by dissolved O_2. This can be attributed to reduced degradation of the conducting salt using X-ray photoelectron spectroscopy. In addition, freshly deposited lithium is compared to a commercial lithium foil. The reactivity of the native passivation layer on the lithium foil differs significantly from freshly deposited lithium with respect to the influence of dissolved O_2, which is a possible reason for the apparently contradictory statements in the literature.

Overall, the results obtained in this work significantly improve the understanding of the interaction between dissolved O_2 and the lithium metal anode. Furthermore, the results are not only relevant for research on Li–O_2 batteries, but also of interest for other metal–O_2 batteries or lithium metal batteries.

Zusammenfassung

Aprotische Li–O_2-Batterien gelten als vielversprechende Energiespeicher für mobile Anwendungen, da sie eine hohe theoretische Energiedichte aufweisen, die deutlich über der von Lithium-Ionen-Batterien nach dem aktuellen Stand der Technik liegt. Sie sind jedoch noch weit von der Kommerzialisierung entfernt, da sie unter einer geringen Lebensdauer und einer hohen Ladeüberspannung leiden. Ein weiters Problem sind zahlreiche Degradationsreaktionen, von denen viele im Zusammenhang mit gelöstem O_2 stehen. Diese Arbeit untersucht den Einfluss von im Flüssigelektrolyten gelöstem O_2 auf die Lithiumanode, der in der Literatur bisher nicht geklärt werden konnte.

Zunächst wird eine systematische Studie über die Löslichkeit und Diffusion von O_2 in verschiedenen Elektrolyten durchgeführt. Zur Bestimmung des Diffusionskoeffizienten werden sowohl ein experimenteller Ansatz als auch molekulardynamische Simulationen verwendet. Dabei wird eine gute Übereinstimmung zwischen Theorie und Experiment festgestellt, was zeigt, dass beide Methoden für die Bestimmung des Diffusionskoeffizienten geeignet sind. Darüber hinaus wird eine Korrelation zwischen der experimentell ermittelten O_2-Löslichkeit und der Oberflächenspannung des Lösungsmittels hergestellt, was in Zukunft die Vorhersage der O_2-Löslichkeit in anderen Lösungsmitteln ermöglicht. Insgesamt reduzieren diese Erkenntnisse den Arbeitsaufwand zur Bestimmung von O_2-Löslichkeit und -Diffusivität erheblich und ermöglichen somit den Transfer der Ergebnisse zu anderen Elektrolyten.

Da bislang aufgrund widersprüchlicher Literatur unklar war, ob sich gelöstes O_2 positiv oder negativ auf die Stabilität der Lithium-Metall-Anode auswirkt, wird diese Fragestellung weiter untersucht. Lithium Abscheidungs- und Auflösungsexperimente zeigen, dass die Coulomb-Effizienz durch gelöstes O_2 deutlich erhöht werden kann. Das kann mit Hilfe von Röntgen-Photoelektronenspektroskopie auf eine verringerte Degradation des Leitsalzes zurückgeführt werden. Darüber hinaus wird frisch abgeschiedenes Lithium mit einer kommerziellen Lithium-Folie verglichen. Die Reaktivität der nativen Passivierungsschicht auf der Lithium-Folie unterscheidet sich in Bezug auf den Einfluss von gelöstem O_2 deutlich von frisch abgeschiedenem Lithium, was eine mögliche Ursache für die scheinbar widersprüchlichen Aussagen in der Literatur ist.

Insgesamt können die in dieser Arbeit erzielten Ergebnisse das Verständnis der Wechselwirkung zwischen gelöstem O_2 und der Lithium-Metall-Anode erheblich verbessern. Darüber hinaus sind die Ergebnisse nicht nur für die Forschung an Li–O_2-Batterien relevant, sondern auch für andere Metall–O_2-Batterien oder Lithium-Metall-Batterien von Interesse.

Contents

1 Introduction

In recent years, we have been increasingly confronted with the consequences of climate change in the form of extreme weather events and an increase in temperature. In order to slow down climate change, greenhouse gas emissions have to be minimized. Therefore, energy production has to shift from fossil fuels to renewable energies. In Germany in particular, a relevant share of CO_2 emissions is attributable to the transport sector. Unfortunately, in contrast to many other sectors, no significant improvements have been achieved in this area. Emissions here have even risen minimally in the last two years.[1] In order to achieve the emission target of Germany being climate neutral by 2045,[2] however, the transport sector will also have to make its contribution. For this, it is imperative to replace combustion engines with electric vehicles. In addition to the legal basis, it is important to improve the acceptance of electric cars in society. Apart from the price, both driving range and charging rate play an important role for this. To ensure that the trend towards more electric cars is sustainable, it is also important to use environmentally friendly and socially compatible materials. For all these factors, the battery is the bottleneck, which means that for the improvement of electric cars, the development of better batteries is the main objective.[3,4]

For a longer driving range, it is necessary to increase the energy density and specific energy of the batteries. However, the lithium-ion batteries (LIBs) that are currently used in electric vehicles have nearly reached their theoretical limit of specific energy, necessitating the need for new energy storage systems.[4,5] One possibility to further improve the energy density is to replace the conventional graphite anode ($Q_{\text{graphite}} = 372\,\text{mA h g}^{-1}$) with a lithium metal anode ($Q_{\text{Li}} = 3860\,\text{mA h g}^{-1}$), resulting in a lithium metal battery (LMB).[6] Another possibility is to use metal–O_2 batteries. These have a particularly high energy density, as they can potentially use O_2 from the ambient air, which does not contribute to the weight of the battery, at least when charged.[3,7] A particularly high theoretical specific energy can therefore be achieved by combining a lithium metal anode with an O_2 cathode ($3485\,\text{W h kg}^{-1}$),[8] which makes Li–O_2 batteries an especially interesting battery system. The specific energy that can be achieved in practical systems is significantly lower, however at an estimated 450–600 W h kg^{-1}[8] it is still higher than that possible by optimizing LIBs ($387\,\text{W h kg}^{-1}$)[9].

However, there are still many obstacles standing in the way of commercializing the Li–O_2 battery: Charging the battery involves a very high overpotential, which leads to poor energy efficiency. In addition, the high voltage required for full charging of the battery can lead to degradation of the cathode and electrolyte. Another problem is the reactivity of various oxygen intermediates present in the battery during cycling, which can also lead to oxidative decomposition of the electrolyte. The use of a lithium metal anode is also associated with challenges, since reactions between lithium metal and the electrolyte can hardly be avoided and lead to the loss of lithium and the electrolyte.[3,10] If the O_2 for cycling is to be supplied from

the ambient air, it must also be taken into account that moisture, CO_2 and N_2 contaminations can also enter the battery.[11] Despite a lot of research on Li–O_2 batteries in recent years, the battery is unfortunately still a long way from actually being used in electric cars or other applications.[3]

In Li–O_2 batteries, the O_2 that is dissolved in the liquid electrolyte can diffuse to and react with the lithium electrode, affecting its stability. The aim of this work is to gain a better understanding of the impact of O_2 crossover on the lithium electrode. In the literature, there have already been various attempts to shed light on the subject, but no clear result has yet been found, as various studies have come to opposite conclusions.[10,12–17] For this purpose, the basics of the Li–O_2 battery (section 2.1) and different models to characterize solubility and diffusivity of gases (section 2.2) are described and the existing literature on O_2 crossover to the lithium electrode (section 2.3) is summarized. Thereafter, the two publications describing the results of this doctoral thesis are presented.

The first publication *"Understanding the Transport of Atmospheric Gases in Liquid Electrolytes for Lithium–Air Batteries"* deals with the solubility and diffusion of the gases O_2, N_2 and CO_2 in different electrolytes that can be used in Li–O_2 batteries (section 3.1). For the experimental determination of the solubility and the diffusion coefficient, gas uptake measurements were carried out. In addition, the diffusion coefficients were calculated by molecular dynamics (MD) simulations. Different models for describing the solubility of gases are used to evaluate the solubilities obtained, which can in the future help to predict gas solubilities in different electrolytes. Furthermore, the experimental and simulated results of the diffusion coefficients were compared and a good qualitative agreement between theoretical and experimental approaches could be found.

In the second publication *"The Influence of Oxygen Dissolved in the Liquid Electrolyte on Lithium Metal Anodes"* the influence of dissolved O_2 on the lithium electrode is then investigated in more detail (section 3.2). For this, lithium plating and stripping in O_2-containing and O_2-free electrolytes were compared. In addition, surface analytics (i.e. scanning electron microscopy (SEM) and x-ray photoelectron spectroscopy (XPS)) were used to compare the morphology and composition of the solid–electrolyte interphase (SEI) from O_2-containing and O_2-free electrolytes. A beneficial influence of dissolved O_2 was found in all experiments. Finally, the surface of the plated lithium was compared with commercial lithium foil and a large influence of the native passivation layer (NPL) on the commercial film was observed. The results obtained in these experiments can help to understand the different contradicting conclusions in the previous literature.[10,13,14]

The present work is a first step towards a better understanding of the influence of O_2 crossover on the lithium electrode. Also the gained knowledge of the solubility and diffusivity of O_2 in the electrolyte leads an important contribution for this. The improved understanding of the positive effect of O_2 but also CO_2 can be important building blocks for the realization of the lithium metal anode in the future.

2 Fundamentals

2.1 The aprotic Li–O_2 Battery

2.1.1 Reactions in Li–O_2 batteries

The aprotic Li–O_2 battery was first described by Abraham and Jiang in 1996. Their electrochemical cell consisted of a lithium metal anode, a polymer electrolyte and a composite carbon cathode in contact to an O_2 permeable membrane. They identified Li_2O_2 as discharge product that was formed via the following overall reaction (equation 1).[18]

$$2\,Li + O_2 \rightleftharpoons Li_2O_2 \qquad E^\circ = 2.96\,V \tag{1}$$

Although different cell architectures of Li–O_2 batteries are possible, this is still the fundamental reaction taking place during charge and discharge. An aprotic Li–O_2 cell consists of a lithium metal anode, an aprotic liquid electrolyte and a porous cathode in contact to an O_2 reservoir (figure 1).

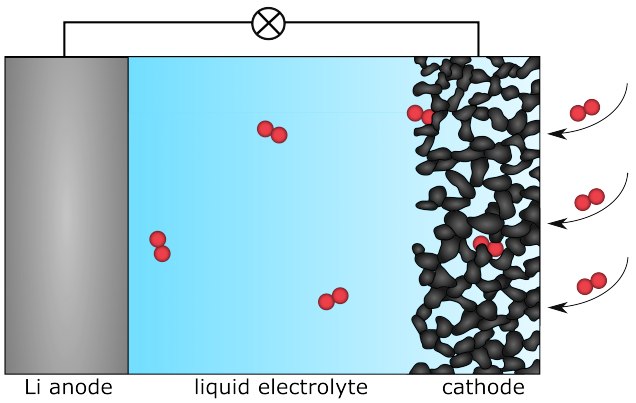

Figure 1: Architecture of a Li–O_2 battery with aprotic liquid electrolyte.

In the conventional aprotic Li–O_2 battery, lithium foil is usually used as anode. Other anode materials such as graphite are theoretically also conceivable. However, lithium metal has the highest possible specific capacity and is therefore the preferred material in terms of energy density ($Q_{Li} = 3860\,mA\,h\,g^{-1}$ vs. $Q_{graphite} = 372\,mA\,h\,g^{-1}$ for LiC_6).[6] On the other hand, lithium metal is strongly reducing and dealing with its high reactivity can be difficult, as further described in section 2.1.2.[6,19] The anode is in direct contact with a Li^+ ion conducting liquid electrolyte which separates anode and cathode from each other. The electrolyte consists of an aprotic organic solvent and a conducting salt. Optionally, a mixture of several solvents or conducting salts, as well as further additives (see section 2.1.3) can be used.[20,21] Also for the cathode, many different types of materials have been

employed. Porous carbon cathodes have, however, become established.[3] To use O_2 as an active material, the battery must be open to an O_2 reservoir so that O_2 can dissolve in the electrolyte and subsequently be reduced at the cathode during discharge. The easiest way to achieve this is with a closed gas reservoir. However, this adds to the total weight of the battery, so it is worthwhile to use O_2 from the ambient air. Unfortunately, this can lead to other problems: Since ambient air contains only 21% O_2, the partial pressure of O_2 is lower, which has consequences for the concentration gradient of O_2 in the electrolyte and the availability of O_2 at the cathode. In addition, volatile solvents can evaporate from the electrolyte when the cell system is open to the outside.[22] Furthermore, H_2O, CO_2 and N_2 can enter the battery from ambient air and react with the anode. CO_2 and H_2O also have a major influence on the discharge mechanism and the stability of the discharge product Li_2O_2, as LiOH and Li_2CO_3 can be formed in side reactions.[8,11,23] This can be partially solved by additional membranes, which are intended to prevent the penetration of e.g. H_2O and the evaporation of the solvent. However, such membranes are still under development.[24]

In order to get a better insight into processes occurring during cycling, it it worth taking a closer look into the discharge process. At the anode, lithium is first oxidized forming Li^+ ions (equation 2) that subsequently migrate through the separator to the cathode.

$$\mathrm{Li} \rightleftharpoons \mathrm{Li^+} + \mathrm{e^-} \tag{2}$$

At the cathode, there are two different mechanisms for the discharge process, which can occur depending on the choice of electrolyte.[25,26] Either way, dissolved O_2 is reduced to $O_2{}^-$ at the cathode surface and recombines with Li^+ to form LiO_2 (equation 3):

$$\mathrm{Li^+} + \mathrm{e^-} + \mathrm{O_2} \rightleftharpoons \mathrm{LiO_2} \tag{3}$$

At this point the mechanism depends on which electrolyte is used. If LiO_2 is not soluble in the electrolyte, it is further reduced at the cathode to form the final discharge product Li_2O_2 (equation 4). This is referred to as the surface-based mechanism.[26]

$$\mathrm{Li^+} + \mathrm{e^-} + \mathrm{LiO_2} \rightleftharpoons \mathrm{Li_2O_2} \tag{4}$$

However, if LiO_2 is soluble in the electrolyte, LiO_2 can disproportionate to Li_2O_2 and O_2 in the solution-based mechanism.[26,27]

$$2\,\mathrm{LiO_2} \rightleftharpoons \mathrm{Li_2O_2} + \mathrm{O_2} \tag{5}$$

As mentioned before, which mechanism takes place depends on the LiO_2 dissolving ability of the electrolyte. For this property, the solvents Lewis basicity is relevant, which can be quantified using the Gutmann donor number (DN). In solvents with a high DN, i.e. strong Lewis bases such as dimethyl sulfoxide (DMSO), LiO_2 is soluble and the solution-based mechanism takes place.[26] Solvents with a low DN such as acetonitrile (MeCN), however, lead to the surface-based discharge mechanism.[27] Furthermore, the discharge mechanism can be influenced by the current density. At high current densities, even in solvents with a high DN, LiO_2 is directly reduced at the cathode in the surface-based mechanism (equation 4).[28,29]

Which of the two mechanisms takes place has a great influence on the morphology and distribution of the discharge product. Since the LiO_2 cannot be transported away from the cathode in the surface-based mechanism, Li_2O_2 forms as a thin film where the O_2 was initially reduced. Due to the poor electrical conductivity of Li_2O_2, this passivates the cathode resulting in a rather low discharge capacity. In the solution-based mechanism however, transport of LiO_2 through the electrolyte

leads to a better distribution of Li_2O_2 that precipitates as larger toroidal particles. Consequently, a higher utilization of the cathode and an improved discharge capacity can be achieved.[27,28]

Since no LiO_2 could be detected as intermediate during charging, it can be assumed that charging does not occur in a reversed way of the discharge mechanism. Hence, the transfer of two electrons is required for the electrochemical decomposition of Li_2O_2 (equation 6).[25]

$$Li_2O_2 \longrightarrow O_2 + 2\,Li^+ + 2\,e^- \tag{6}$$

However, the oxygen evolution reaction (OER) is associated with a very high overpotential.

2.1.2 Limitations of Li–O_2 batteries

Overall, the Li–O_2 battery promises many advantages, especially in terms of energy density and specific energy. However, the commercialization of Li–O_2 batteries is still hindered by major challenges and limitations.[3,10,30] As shown in figure 2, these problems can be divided into three categories: lithium metal anode related limitations, cathode related limitations and electrolyte degradation.

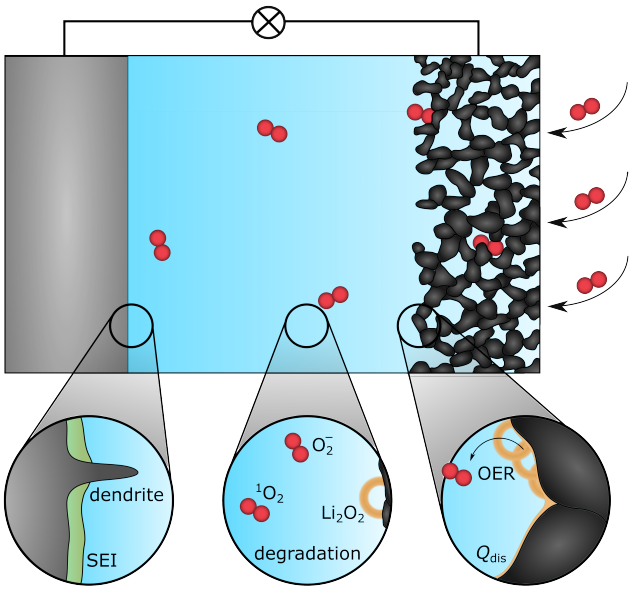

Figure 2: Challenges of Li–O_2 batteries including anode related limitations, cathode related limitations and electrolyte stability.

The use of a lithium metal anode is indispensable when aiming for the highest possible energy densities, but it also brings many challenges.[6] The strongly reducing nature of lithium leads to side reactions with the electrolyte. This applies to both the solvent and the conducting salt, as well as species dissolved therein, such as O_2 or additives.[6,19,31] All side reactions with the lithium metal anode result in a loss of lithium and thus a loss of capacity. Therefore, lithium must be used in excess, which in turn increases the weight of the battery.[3,6] The same applies to the electrolyte, as drying out of the battery due to loss of solvent in side reactions should be prevented. In addition, the reductive decomposition of the electrolyte causes a layer of side reaction products to form at the SEI. Ideally, this SEI should completely cover the lithium metal anode so that further side reactions are prevented

by passivation of the electrode. In addition, the SEI must have a high degree of flexibility and mechanical stability to prevent cracking. However, ensuring stable SEI during cycling is difficult because the volume of the electrode changes significantly during plating and stripping of lithium.[6,19,32] In addition, lithium is not always deposited homogeneously and dendrites tend to form during lithium plating. An inhomogeneous SEI can intensify this effect, since there is preferential deposition of lithium in cracks in the SEI.[33] The dendrites can grow through the separator to the cathode and thus create a short circuit. This is not only detrimental for the battery, but also poses a significant safety risk.[3,6,19]

At the cathode, there are also challenges that need to be overcome: One of the main problems is that the discharge product is not well distributed in the cathode, which reduces the discharge capacity. This may be due to the discharge mechanism. When the surface-based mechanism takes place, only a thin film of Li_2O_2 can be formed on the cathode before the low conductivity of Li_2O_2 prevents further discharging.[8] Furthermore, pores of the cathode can be clogged by Li_2O_2 and are then no longer available as electrochemically active surface.[8] Moreover, the majority of Li_2O_2 is often deposited at the O_2 reservoir-facing side of the electrode, so that only a fraction of the electrode is utilized. Due to the sluggish diffusion of O_2 through the electrolyte, the reduction of O_2 directly occurs at the outer parts of the electrode and O_2 cannot penetrate the whole cathode because diffusion paths become too long.[34] In addition, the dissolution of the Li_2O_2 during charging is associated with a very high overpotential which reduces the energy efficiency of the battery.[35] Furthermore, the high voltage that has to be applied for this can lead to degradation of the carbon cathode.[36] Another problem is the high reactivity of the Li_2O_2. Side reactions can occur both at the Li_2O_2–electrolyte interface and at the Li_2O_2–electrode interface (equation 7). This results in the formation of a Li_2CO_3 film on the Li_2O_2 surface which increases the overpotential during charging and makes it even more difficult to fully charge the battery.[37]

$$2\,Li_2O_2 + 2\,C + O_2 \longrightarrow 2\,Li_2CO_3 \tag{7}$$

Furthermore, degradation of the electrolyte is another challenge. There are extremely high requirements for the stability of the electrolytes in Li–O_2 batteries. On the one hand, the electrolyte must be sufficiently stable towards the lithium metal anode.[6] Secondly, it must also be stable towards reactive oxygen species (e.g. $^1O_2$[38–40], O_2^-[41] and also Li_2O_2[37]) in order to avoid oxidative decomposition. Although this applies to all electrolyte components, the following section will focus on solvents.

Reductive decomposition can be observed to some extent in all electrolytes. In ether and carbonate based electrolytes, a covering SEI of insoluble reaction products (e.g. LiOH, Li_2O, Li_2CO_3, LiOR, LiOOCR) can form, protecting the anode from further reactions.[32] For DMSO, MeCN or amide based electrolytes, however, such a protective SEI can usually not be observe.[20,42] In order to obtain a more stable SEI, SEI forming additives are of particular importance in these electrolyte systems.

Ethers are the solvents that are considered the most stable towards reduction at the lithium metal anode.[20,21] However, they are prone to oxidative decomposition. The proposed mechanism of ether decomposition by O_2 is shown in figure 3.[41] Apart from O_2, oxidative decomposition reactions can also involve O_2^-, Li_2O_2 and $^1O_2$. The superoxide radical anion O_2^- for example is both a very strong nucleophile and a strong base. Degradation of the solvents can therefore take place by acid-base reactions and by nucleophilic attacks.[26,31] Especially DMSO (S=O) and carbonyl compounds (C=O) that are for example present in carbonates are susceptible to

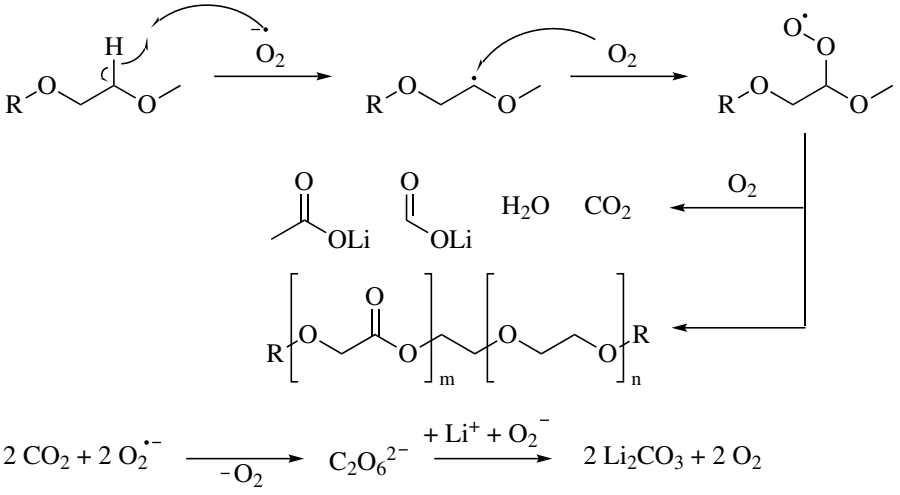

Figure 3: Decomposition mechanism of ether-based solvents by O_2^{-}.[41]

nucleophilic attacks by O_2^{-}.[43] For the stability of ionic liquids (ILs), on the other hand, the basic nature of O_2^{-} is the main problem, since O_2^{-} can abstract a proton from many organic cations in an acid-base reaction and thus lead to degradation of the IL.[44,45] Also $^1O_2$, which can form during cycling, is discussed as a source of detrimental side reactions as it is highly reactive.[38–40]

2.1.3 Electrolyte design

Many of the challenges mentioned in section 2.1.2 can be addressed by a tailored design of the electrolyte. An important point is, of course, the selection of the solvent and the conducting salt. Another strategy is the addition of electrolyte additives.

The solvents used are mainly various ethers and amides, as well as DMSO and MeCN.[20,21] Carbonates, which are common in LIBs, are usually not employed because they do not have sufficient stability against reactive oxygen species, especially O_2^{-}.[46,47] When selecting the solvent, stability is the most important factor, as it is crucial for safety and the lifetime of the battery. Since the discharge mechanism and thus the discharge capacity depend to a large extent on the DN of the electrolyte, this should also be taken into account.

The most commonly used conducting salts are lithium bis(trifluoromethanesulfonyl)imide (LiTFSI), lithium bis(fluorosulfonyl)imide (LiFSI), lithium triflate (LiOTf), $LiNO_3$, $LiClO_4$, $LiPF_6$ $LiBF_4$ and lithium bis(oxalato)borate (LiBOB). However, most of these salts are not completely stable and are decomposed at the anode.[48] However, a limited amount of degradation is often accepted in order to specifically improve the properties of the SEI, e.g. by increasing its LiF-content. Another strategy to protect the anode is to use high concentrations of the conducting salt. By increasing the salt concentration, fewer solvent molecules per ion are available for solvation. This leads to anions and cations sharing parts of the solvate shell (shared solvent ion pair; SSIP) or even being in direct contact with each other (contact ion pair; CIP) as depicted in figure 4. In these so-called solvent-in-salt electrolytes, there are no free solvent molecules left that are not involved in the solvation of ions. Therefore, detrimental side reactions of the solvent are strongly reduced. This especially applies to reactions with the anode, which is reflected in a much more homogeneous and stable SEI.[49–51]

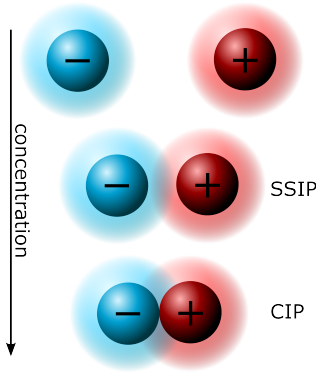

Figure 4: Schematic depiction of SSIP and CIP.

Another possibility is to use SEI-forming additives. These are compounds that are added to the electrolyte in low concentrations to react with the anode, thereby improving the properties of the SEI. Some additives, such as fluoroethylene carbonate (FEC)[52] and vinylene carbonate (VC)[53], are already known from LIBs and LMBs. FEC is particularly popular because it leads to a stable LiF-rich SEI. However, when used in combination with a lithium metal anode, FEC is often consumed continuously, requiring high concentrations.[6] Additionally, it is unclear whether these findings can be transferred to Li–O_2 batteries since most studies on SEI-forming additives for lithium electrodes involve LMBs and it is unclear whether their efficacy is affected by the presence of dissolved O_2.

Furthermore, the stability of the electrolyte and the cathode can be improved by quenching reactive intermediates. For example, to prevent degradation by $^1O_2$, 1-pentyl-1,4-diazabicyclo[2.2.2]octan-1-ium (DABCOnium) can be added as a singlet quencher, which significantly increases the lifetime of the cells.[54] However, this approach is more difficult with other reactive species. Since the presence of O_2^-, for example, is relevant for the discharge process, it cannot simply be quenched.

The high charge overpotential is another problem that can be solved by using electrolyte additives that assist the OER. Redox mediators (RM) are compounds that can be oxidized at a redox potential that is slightly higher than the standard potential of the Li–O_2 battery (2.96 V)[18]. When charging the battery, this reaction takes place forming the oxidized form of the RM (RM^{ox}) as shown in equation 8.

$$2\,\mathrm{RM} \rightleftharpoons 2\,\mathrm{RM^{ox}} + 2\,\mathrm{e^-} \tag{8}$$

Subsequently, the oxidized RM can chemically react with precipitated Li_2O_2 forming O_2 and recover the RM (equation 9).

$$\mathrm{Li_2O_2} + 2\,\mathrm{RM^{ox}} \rightleftharpoons \mathrm{O_2} + 2\,\mathrm{Li^+} + 2\,\mathrm{RM} \tag{9}$$

This reduces the voltage required to charge the battery to a value close to the redox potential of the RM. The lower voltage during charging improves the energy efficiency of the battery and prevents cathode degradation, which occurs at high voltages. Moreover, this enables the decomposition of Li_2O_2 without direct contact to the cathode, which would not be accessible for electrochemical reactions.[55–57] The disadvantage of many RMs, however, is that the stability towards the lithium electrode or reactive oxygen intermediates is not yet sufficient and the RMs degrade after a few cycles.[58–61]

RMs can also be used for the oxygen reduction reaction (ORR) during the discharge process of Li–O_2 batteries, in order to enable the solution-based discharge

mechanism even in solvents that do not dissolve LiO_2. This can prevent film growth of Li_2O_2 and passivation of the electrode and thus increase the discharge capacity. In addition, a higher current density can be achieved during discharge.[62]

Another way to improve the discharge capacity is to improve the O_2 solubility or diffusivity in the electrolyte. With more dissolved O_2, a larger part of the cathode can be utilized. Furthermore, improved O_2 transport allows higher current densities (see section 2.2.2). To achieve this, additives such as perfluorocarbons (PFCs), that have a particularly high gas solubility, can be used.[63–65]This demonstrates that O_2 solubility and diffusion are important parameters for Li–O_2 electrolytes. Therefore, they will be explained in following section in more detail. Furthermore, it will be discussed which other possibilities there are to specifically influence gas solubility and diffusion in order to obtain optimized electrolytes.

2.2 Diffusivity and Solubility of Gases in Liquids

For Li–O_2 batteries, O_2 solubility and diffusivity are important electrolyte parameters. Since O_2 is the active material at the cathode, O_2 transport through the electrolyte is a crucial factor for the limiting current density. For the selection of the electrolyte, this means that the highest possible O_2 solubility and diffusivity should be aimed for, if high rates are required.

Also for the SEI formation at the anode, solubility and diffusivity of several gases are relevant, since they can diffuse to the anode and be involved in side reactions there. This also applies to all gases that emerge from degradation of cathode or electrolyte. CO_2 for example can be formed by oxidative degradation of cathode[36] or electrolyte[41] and is therefore often present in the electrolyte. Additionally, in Li–air batteries, N_2 from ambient air might also be dissolved in the electrolyte and can influence the SEI as well.[17,30]

This chapter summarizes models that are used to describe the solubility and diffusivity of gases in liquids and how they can be used for designing electrolytes with improved gas transport properties.

2.2.1 Models to Describe Gas Solubility in Liquids

There are several ways of describing the solubilities of gases in liquids. One of them is Henry's law. Henry's law solubility constant H^{cp} is expressed as the ratio of the concentration of a dissolved gas in the liquid phase $c_{\text{gas}}^{\text{sol}}$ to the partial pressure of this gas in the atmosphere above the liquid p_{gas}:[66]

$$H^{cp} = \frac{c_{\text{gas}}^{\text{sol}}}{p_{\text{gas}}} \tag{10}$$

This representation is convenient because it allows direct calculation of the gas concentration in the electrolyte at a given partial pressure of the respective gas.

Another way of describing the gas solubility in a liquid is through the Ostwald coefficient L. It is defined as the ratio of the gas volume V_{gas} to the volume of the solvent needed to dissolve it V_{sol} (equation 11). This is equivalent to the ratio of the concentration of a dissolved gas in the solvent $c_{\text{gas}}^{\text{sol}}$ to the concentration of the respective gas in the gas phase $c_{\text{gas}}^{\text{atm}}$:

$$L = \frac{V_{\text{gas}}}{V_{\text{sol}}} = \frac{c_{\text{gas}}^{\text{sol}}}{c_{\text{gas}}^{\text{atm}}} \tag{11}$$

Formally, the Ostwald coefficient is the equilibrium constant of gas solvation. If $L > 1$, there is more gas dissolved in a liquid than in the pure gas phase with the same volume.[66]

In order to better understand gas solubility and to assess the factors on which it depends, various models have been developed. The two most relevant of these are the regular solution theory and the cavity model. However, the regular solution theory is limited to non-polar solvents and solutes. While acceptable predictions can be made in slightly polar solvents, the regular solution theory cannot be applied to polar solvents such as DMSO.[66,67]

The cavity model is therefore more suitable for describing the solubility of gases in solvents that are relevant for Li–O_2 batteries. According to this model, the solution of a gas in a pure solvent can be divided into two steps: First a cavity of the size of

the solute atom or molecule has to be created. For this, work has to be carried out against the surface tension σ of the solvent. Second, the solute is inserted into the cavity, resulting in a gain in interaction energy E between solute and solvent. For a spherical solute with radius r, the Ostwald coefficient L at a given temperature T can then be described as in equation 12 with k_B as the Boltzmann constant:[68]

$$\ln L = -\frac{4\pi r^2 \sigma + E}{k_B T} \tag{12}$$

Assuming that E is independent of the solvent, a linear relationship between $\ln L$ and σ is obtained. When plotting $\ln L$ against σ, E can be determined from the y-axis intercept and r from the slope of a linear regression.[68] The solubility of O_2 in various solvents was evaluated accordingly in the first publication (see section 3.1).[69] As a result, the gas solubility in solvents whose surface tension is known can be predicted on the basis of a few data points. Since the surface tension of many solvents is tabulated, this considerably reduces the effort required to estimate the gas solubility. Accordingly, particularly good O_2 solubility can be achieved in solvents with very low surface tension. This is the case, for example, with PFCs, which have a low surface tension due to weak intermolecular interactions and therefore exhibit excellent gas solubilities.[70,71]

Despite the criticism that the model does not take into account a change of E in different solvents and uses bulk surface tension, which does not seem to be suitable for molecular-sized cavities,[66] it works very well for a variety of different gases in pure solvents. This is shown by the fact that the quality of linear fits is mostly very good. Also the solute radii calculated with the the slope agree well with the van der Waals radii determined by other methods (e.g. calculated from the co-volume b).[68]

However, the model reaches its limits when a mixture (e.g. an electrolyte with solvent and conducting salt) is used instead of a pure solvent. On the one hand, it is questionable whether it can still be assumed that E remains constant. On the other hand, the work required to generate the cavity is poorly described by the bulk surface tension of a mixture, since the component with the lower surface tension accumulates on the surface.[66] Therefore, to understand how gas solubility is affected by the addition of conducting salts, other explanatory approaches are required, which are described in the following:[66,72]

The first way of describing the salt effect relates to the hydration or solvate shell. When dissolving a salt, solvent molecules are needed to form a solvate shell. These molecules are then no longer available to solvate other components, e.g. gases, resulting in a decrease in gas solubility compared to the pure solvent (the so-called salting-out effect).[66] In some systems, however, the gas solubility can also increase (salting-in effect), which cannot be explained by this model.[66,73]

The second model is the electrostatic theory that relates the gas solubility to the dielectric constant of the solution. According to Debye's model, a non-electrolyte solute is salted-out when it reduces the total dielectric constant of the solvent. If it increases the dielectric constant, it is salted-in.[74] For this, the solute has to have a higher total molecular polarization than the solvent, which is not the case for gases like O_2 in common organic solvents. Therefore, O_2 should be salted-out according to Debye, which is however not the case in all electrolytes.[75]

In the van der Waals theory, the electrostatic model is extended by including dispersion forces. Lyotropic salting-in occurs when the electrostatic salting-out effect is exceeded by dispersion salting-in. Lyotropic salting-in is mainly observed in electrolytes with very large ions.[73] As salting-in of O_2 in electrolytes can be understood as lyotropic salting-in, O_2 solubility in a given solvent can be modified by the size of the anion of the conducting salt. As example, the solubility of O_2 in different

diethylene glycol dimethyl ether (diglyme)- and DMSO-based electrolytes is given in figure 5. In both solvents, lithium sulfonylimides with differently sized fluorinated

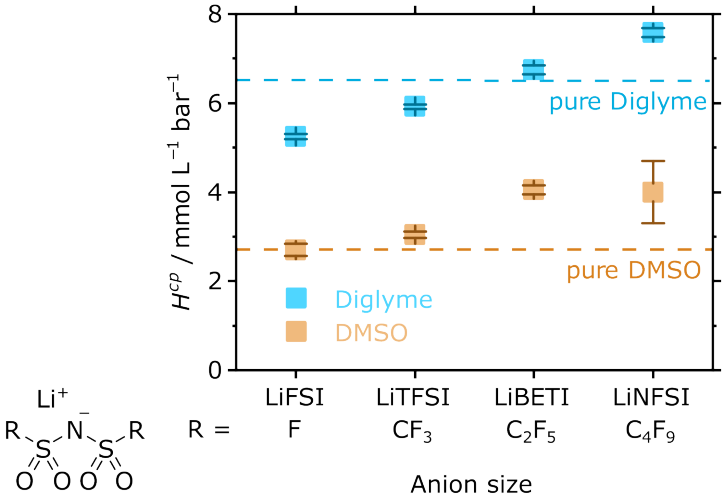

Figure 5: O_2 solubility in diglyme- an DMSO-based electrolytes in dependence of anion size. Data for diglyme-based electrolytes taken from [76].

alkyl chains (LiFSI, LiTFSI, lithium bis(pentafluoroethanesulfonyl)imide (LiBETI) and lithium bis(nonafluorobutanesulfonyl)imide (LiNFSI)) were used as conducting salt. The solubility of O_2 can be significantly increased when larger anions are used.

Lastly, salting-out and salting-in effects can be described by the internal pressure of a salt solution that is related to changes in both volume and compressibility.[72]

Overall, this section shows that the understanding of the gas solubility and the factors that can be used to influence it enable the tailored modification of electrolytes, e.g. to achieve a higher O_2 solubility. In pure solvents, the cavity model can even be used to make a quantitative prediction. Although it is difficult to make quantitative statements about the solubility in electrolytes with conducting salt, the effect of different conducting salts on the gas solubility in the electrolyte can be qualitatively compared very well. In addition, solvents and conducting salts can be specifically selected with regard to their gas solubility.

2.2.2 Models to Describe Diffusion of Gases in Liquids

The solubility can be used to calculate the maximum concentration of a gas in the electrolyte that can be achieved at a given pressure. However, to determine the actual local concentration of the gases at the electrodes, knowledge of the diffusivity is also necessary. During discharge for example, O_2 is consumed at the cathode. To replenish the O_2, it must be transported from the boundary to the gas phase to the electrode through the electrolyte by diffusion. Side reactions at the anode also consume the respective gas (e.g. O_2, N_2 or CO_2) and the rate at which these reactions occur depends critically on how fast diffusion through the electrolyte to the anode can take place.

Any reaction involving a dissolved gas leads to the formation of a concentration gradient $\frac{\partial c}{\partial x}$, since the dissolved gas is depleted at the electrode. The resulting flux j of the dissolved component with a diffusion coefficient D towards the electrode can be described by the one-dimensional case of Fick's first law (equation 13). The minus

sign indicates that diffusion takes place in the direction of the lower concentration.

$$j = -D\frac{\partial c}{\partial x} \tag{13}$$

In a Li–O_2 battery with a planar cathode, for example, the transport of O_2 can be considered as constant diffusion through a thin film between electrode and electrolyte surface. According to the Nernst diffusion layer model, the O_2 concentration at the electrode is 0, since it is completely consumed there. At the electrolyte surface, the O_2 concentration $c_{O_2}^{sol}$ is determined by Henry's law solubility constant H^{cp} and the partial pressure of O_2 in the gas reservoir above the electrolyte p_{O_2}. With these boundary conditions, equation 14 can be derived from equation 13 with δ as the thickness of the Nernst diffusion layer:

$$\begin{aligned} j_{O_2} &= -D_{O_2}\frac{c_{O_2}^{sol}}{\delta} \\ &= -D_{O_2}\frac{H_{O_2}^{cp} p_{O_2}}{\delta} \end{aligned} \tag{14}$$

The resulting O_2 concentration gradient is depicted in figure 6:

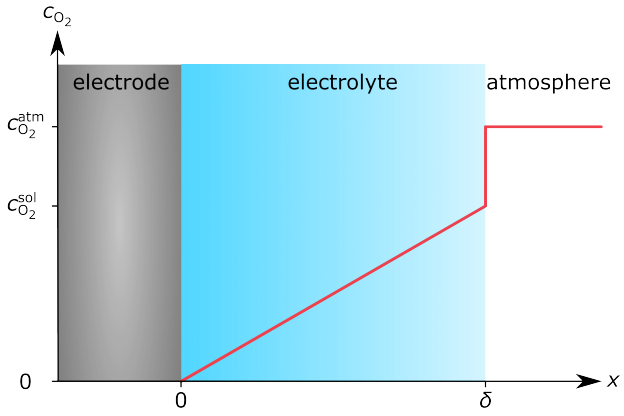

Figure 6: Concentration gradient of O_2 during discharge of a Li–O_2 battery with a planar cathode according to the Nernst diffusion layer model.

From this, the limiting current I_{lim} that can be achieved during discharging can be derived as shown in equation 15 with n as the number of transferred electrons, F as the Farady constant and A as the electrode surface.

$$I_{lim} = \frac{nFAD_{O_2}H_{O_2}^{cp}p_{O_2}}{\delta} \tag{15}$$

In this model with a two-dimensional electrode, the limiting current is therefore proportional to both D_{O_2} and $H_{O_2}^{cp}$ and can be influenced equally by both parameters. In addition, the limiting current can be increased by reducing δ or increasing A or p_{O_2} [77].

It has to be noted that real cathodes often have a three-dimensional structure with pores etc. and are therefore more complex. The model with planar electrodes can therefore only be used to a limited extent for the consideration of the O_2 concentration gradient. As a result, there are large differences in the local O_2 concentration: Since O_2 is consumed at the cathode, the concentration is highest on the side of the cathode facing the O_2 reservoir. This leads to the fact that Li_2O_2 is preferentially formed there and the cathode surface cannot be utilized homogeneously,

especially at high current densities.[34] Also other factors such as pore clogging have to be taken into account.[78] When considering three-dimensional electrodes, it is especially important to have fast O_2 diffusion to facilitate a homogeneous utilization of the cathode. It is therefore desirable to gain a better understanding of the parameters on which the diffusion coefficient of O_2 depends.

According to the Einstein–Smoluchowski relation the diffusion coefficient of a component can be formulated in dependence of its mobility μ:

$$D = \mu k_B T \tag{16}$$

For the diffusion of uncharged spherical particles with radius r, this gives the Stokes–Einstein equation with η as the dynamic viscosity of the liquid:

$$D = \frac{k_B T}{6\pi\eta r} \tag{17}$$

The diffusivity of different gases is therefore antiproportional to their radius. According to this model, the only electrolyte property that influences the diffusivity of a given gas is therefore the dynamic viscosity, which is anti-proportional to the diffusion coefficient. If a high O_2 diffusivity is desired to achieve high rates and a high cathode utilization, the viscosity should therefore be as low as possible. However, the diffusion coefficients of all other components dissolved in the electrolyte are increased similarly by a low η, which may also accelerate side reactions at the anode. As a consequence, high concentrations of conducting salts, which increase the electrolytes viscosity, decreases the diffusion coefficient of all components in this electrolyte. Highly concentrated electrolytes are considered to have great potential as they can have a beneficial influence on SEI properties (see section 2.1.3). However, it should be noted that the diffusion of O_2 is particularly slow in electrolytes in which CIPs or SSIPs are formed. This shows that it is generally important to consider various aspects when developing and optimizing electrolytes. The diffusion and solubility of O_2 should not be lost sight of, as they are decisive for the limiting current density as well as for the cathode utilization and thus for the discharge capacity.

2.3 Crossover

2.3.1 Interaction of different side reactions

As described in section 2.1.2, there are a number of possible side reactions and degradation mechanisms in Li–O_2 batteries that can affect all cell components. Often they are divided into cathode, anode and electrolyte degradation and the different problems are considered separately. However, it is also possible that different degradation reactions influence each other, if products from side reactions trigger further degradation elsewhere. These synergistic effects are less often considered in the literature than degradation of the individual components, although the interaction of anode, cathode and electrolyte is also very important for the stability of the Li–O_2 battery.[31] Therefore, the various possible synergistic effects between cathode, anode and electrolyte will be discussed in the following.

In general, the electrolyte of a Li–O_2 battery contains the electrolyte components, such as the solvent, the conducting salt (or a mixture of several different solvents or conducting salts), and various additives, as described in section 2.1.3. In addition, there is dissolved O_2 and possibly other dissolved gases from the ambient air (see section 2.2.1). Further components can be formed by known side reactions, which must be taken into account in subsequently: A reductive decomposition of the electrolyte takes place at the lithium metal anode, whereby the SEI consisting of inorganic (LiF, Li_2O, Li_2CO_3) and organic (ROLi, RCOOLi, polymers) components is formed as a solid layer on the lithium metal anode. However, soluble components can also be formed, which can be transported through the electrolyte. Furthermore, the electrolyte is oxidatively decomposed by dissolved O_2 or other reactive oxygen intermediates, producing CO_2 and other mostly organic electrolyte fragments. Degradation of the cathode, e.g. by high charging overpotentials, also leads to the formation of CO_2, which is then dissolved in the electrolyte. Subsequently, all of these components can trigger further degradation reactions. An example of the synergy between electrolyte and anode degradation is that the SEI component Li_2O is a strong base and can deprotonate solvents such as DMSO, leading to increased decomposition of the electrolyte.[79]

Because of their direct contact, it is obvious that there is some interaction between the anode and the electrolyte, or between the cathode and the electrolyte, and thus a connection between the degradation reactions associated with the respective cell components. What is less often considered is the synergy between cathode and anode, since these are separated by the electrolyte. However, if soluble components are formed in reactions at the electrodes, they can diffuse through the electrolyte to the other electrode and interact with it.

A very well-known example of the crossover problem are RMs, which can be used as electrolyte additives to catalyze OER or ORR (see section 2.1.3). By default, these molecules have an oxidized and a reduced form that is soluble in the electrolyte. After the RM is oxidized at the cathode, it is therefore possible that it migrates to the anode and is reduced there. The reduced form can then migrate back to the cathode, and the RM thus serves as a redox shuttle between anode and cathode. As a result, the battery continuously discharges itself both during cycling and without current flow, if crossover of the RM is not prevented.[61,80–82]

Another example is the crossover of degraded cathode components to the anode. In a paper by Younesi *et al.*, degraded components of the binder used at the cathode were found to be components of the SEI on the lithium metal anode after cycling. It was concluded that the binder is first decomposed at the cathode and that soluble or

mobile products of this degradation reaction can subsequently diffuse to the anode and are there incorporated in the SEI.[83]

For this work, however, it is particularly relevant that the gases dissolved in the electrolyte at the cathode can also diffuse to the anode and react there. In the case of O_2, this is explained in detail in the following section (2.3.2). But also CO_2 or N_2 can significantly influence the composition of the SEI at the anode.

2.3.2 Oxygen Crossover to the Anode

It has been known for many years that O_2 dissolved in the electrolyte has an influence on the lithium electrode. Nevertheless, there have been only a few studies on this topic so far. In addition, the authors of these studies disagree as to whether O_2 has a positive or negative influence on the lithium electrode, and there have only been few attempts to explain the cause of the different results in the literature. In the following, the studies that have dealt with this topic so far will be described in more detail.

Aurbach *et. al.* conducted the first investigation on the impact of O_2 contamination in the electrolyte on lithium electrodes in 1989. The researchers observed an improvement in the cycling efficiency of the lithium electrode in all the examined electrolytes, namely γ-butyrolactone, propylene carbonate (PC), and tetrahydrofurane (THF) with $LiClO_4$ and $LiAsF_6$. They concluded that dissolved O_2 reacts more quickly with the lithium electrode than the electrolyte, leading to the formation of an oxide-based protective film that reduces overpotential and dendrite formation during cycling. They demonstrated, through SEM images, that fewer dendrites were formed on the electrodes cycled in O_2-containing electrolytes.[84] However, a comparison with later studies is difficult, since now mainly ether- or DMSO-based electrolytes are applied in Li–O_2 batteries instead of the electrolytes used in this study.

Assary *et al.* then brought attention to the issue of O_2 crossover in Li–O_2 batteries again in 2012. Through the use of *in situ* x-ray diffraction (XRD), they demonstrated the formation of LiOH and Li_2CO_3 on the lithium electrode during cycling of Li–O_2 cells with LiOTf in tetraethylene glycol dimethyl ether (tetraglyme) as the electrolyte. Additionally, they conducted DFT studies of ethers in an O_2 environment and proposed a similar decomposition mechanism as Freunberger *et al.*[41] to explain the influence of O_2 on the SEI via the decomposition of ethers. However, since they investigated Li–O_2 full cells, the comparison to O_2-free electrolytes was missing and they did not provide experimental evidence, that these reactions are indeed triggered by dissolved O_2 and do not occur in e.g. argon atmosphere.[13]

In 2014, Lee *et al.* conducted a study on Li–Li symmetrical cells, using 1.15 M LiTFSI in DMSO as the electrolyte. They compared cells cycled in an argon and O_2 atmosphere, utilizing XPS, SEM, electrochemical impedance spectroscopy (EIS), Fourier transform infrared spectroscopy (FT-IR), and symmetrical cell cycling. Through EIS, they analyzed the chemical degradation of lithium electrodes and discovered that in the O_2-free electrolyte, a maximum impedance was attained after three days, followed by a constant impedance due to the formation of a stable SEI. In contrast, the impedance constantly increased in the O_2-containing electrolyte, indicating an unstable or incompletely covering SEI that facilitates continuous chemical decomposition of the lithium electrode. The researchers compared SEM images of the stored lithium electrodes to support their findings, which revealed that the O_2-free electrolyte preserved a flat, homogeneous surface, whereas the O_2-containing electrolyte led to a rugged and moss-like lithium surface. XP spectra of the stored electrodes exhibited significantly more sulfur-containing species, including

SO_4^{2-}, SO_2, S=O, and S^{2-}, as well as fluorine and even nitrogen (N–O and Li_3N) species. FT-IR spectra yielded the same results. Therefore, the authors concluded that dissolved O_2 in the electrolyte induces significant side reactions of the lithium electrode, particularly with DMSO but also with $TFSI^-$. Additionally, they conducted cycling experiments with Li–Li symmetrical cells that exhibited much higher overpotentials and less stable voltage plateaus in the O_2-containing electrolyte. This was the first experimental evidence that in an electrolyte with O_2 more side reactions take place at the lithium electrode.[14]

In contrast to that, Roberts *et. al.* conducted a study on the effects of additives (VC and $LiNO_3$) on the cycling efficiency of lithium electrodes. They investigated the stripping and plating in argon and O_2 atmospheres for DMSO-based electrolytes. According to their findings, the Coulomb efficiency (CE) increased from 25% in the O_2-free electrolyte to 85% in the O_2-containing electrolyte. Therefore, they concluded that O_2 contributes to the formation of a stable and protective SEI that is not established in O_2-free electrolytes.[15] Since they also used a DMSO-based electrolyte, it can be ruled out that the results of Lee *et al.* are only due to the choice of DMSO as solvent.[14,15]

Later, Qiu *et al.* and Wang *et al.* observed that the SEI stability on lithium electrodes stored and cycled in O_2 atmosphere was improved compared to argon atmosphere. They used tetraglyme-based electrolytes in Li–Cu cells and compared lithium stripping and plating while analyzing SEI components with XPS. Both studies concluded that the SEI formed in O_2-free electrolytes contains more decomposition products of the conducting salt, whereas the amount of Li_2CO_3 is increased in the O_2-containing electrolyte. Although the resistance is increased in the electrolyte with O_2, the performance during plating and stripping was improved in O_2 atmosphere due to higher CE, which they explained by decreased lithium loss in side reactions.[16,17] Contrary to the conclusions of Assary *et al.*, there are experiments for ether-based electrolytes that show an improvement of the lithium electrode stability by dissolved O_2. Qiu *et al.* also showed that the CE depends on the availability of O_2 at the electrode. The O_2 reservoir in their setup was on the side of the copper electrode where they deposited lithium. To dissolve as much O_2 as possible in the electrolyte and to optimize the availability at the electrode, they inserted holes in the copper electrode. They observed that the CE increases with more holes and thus better O_2 availability.[16] Hence, O_2 diffusion does not seem to be fast enough to sufficiently protect the lithium electrode without the additional holes. In Li–O_2 batteries, it should also be considered that the battery usually has contact with the O_2 reservoir only at the cathode and the diffusion path to the lithium electrode can therefore be very long. In addition, when discharging, O_2 is consumed at the cathode.

In addition to the studies directly dealing with the influence of dissolved O_2 on the lithium electrode, there are two other publications that actually focus on the comparison of different conducting salts, but also compare O_2-free and O_2-containing electrolytes: Saito *et al.* explored the effects of different conducting salts (LiFSI, LiTFSI, and LiOTf) in tetraglyme-based electrolytes on Li–Li and Li–O_2 cells. Their initial analysis revealed that cell with LiFSI and LiTFSI as conducting salt had higher conductivity than those with LiOTf due to their greater degree of dissociation, which supported the reductive decomposition of anions. However, in symmetrical cells with LiOTf, they observed poor performance and continuous overpotential increase.[85] In addition, they conducted a comparison of symmetrical cells with and without O_2 and found that O_2 improved lithium stripping and plating in the LiOTf electrolyte. Similar to Aurbach *et al.*,[84] they concluded that the direct

reaction of dissolved O_2 with the lithium electrode resulted in the formation of a protective SEI, which prevented the reductive degradation of OTf^- anions.[85]

Tong *et al.* highlighted the importance of selecting the proper conducting salt to suppress harmful O_2-shuttle effects. While their paper primarily focused on promoting lithium (trifluoromethanesulfonyl)(*n*-nonafluorobutanesulfonyl)imide (LiTNFSI) as a superior conducting salt compared to LiTFSI, they also conducted a comparison of symmetric cycling under argon and O_2 atmospheres (albeit at different current densities). Their findings showed that the voltage stability during plating and stripping was notably less consistent in the O_2-containing TFSI-based electrolyte. In the TNFSI-based electrolyte, the overpotential was elevated by dissolved O_2 as well, but only slightly. They also performed SEM, XPS, and differential electrochemical mass spectrometry (DEMS) analyses, and concluded that LiTNFSI produced a thicker, more uniform, and O_2-resistant SEI, along with reduced CO_2 evolution during cycling. In their XP spectra, they observed more C and F for TNFSI, with the difference between TNFSI and TFSI being even more significant in the presence of O_2.[86]

The issue of contradicting literature on this topic was only raised in a review of Liu *et. al.*[10] They pointed out that insufficient O_2 supply to the lithium electrode in some cell architectures might be the reasons for discrepancies in literature, since Qiu pointed out that they observed an influence of O_2 supply on the cycling performance.[16] However, this doesn't explain that some groups observed a decrease in cycling performance in cells with O_2, since Qiu only found less improvement in cells with fewer O_2 compared to the argon reference.

All in all, researchers agree that dissolved O_2 in the liquid electrolyte significantly influences the SEI formed on lithium electrodes, but different researchers come to contradicted results: Assary and Lee show detrimental effects on lithium electrode stability in ether[13]- and DMSO[14]-based electrolytes. In contrast to this, Qiu *et al.*, Wang *et al.* and Roberts *et al.* state that the dissolved O_2 improves SEI stability and lithium cyclability in both of these electrolytes.[15–17] Consequently, the influence of dissolved O_2 in the electrolyte is still unclear and further studies are needed. Moreover, the existing studies focus on many different types of electrolytes which might largely influence the effect of O_2 on the SEI. Therefore, also different solvent and conducting salts, maybe even salt concentrations need to be considered.

Additionally, it is unclear if (significant amounts of) the dissolved O_2 itself reacts with the lithium electrode[84–86] or if the influence of O_2 is mainly due to side reactions with the electrolyte[13,14]. Since dissolved O_2 and other reactive oxygen species that form in O_2-containing electrolyte lead to degradation of the electrolyte, products of this degradation might also react with the lithium electrode and could explain a higher Li_2CO_3 content in the SEI in O_2-containing electrolyte, that can have a beneficial influence on the electrode stability. A simple schematic overview over the possible reactions is shown in figure 7. It also has to be noted that O_2 can be reduced to O_2^- at the lithium electrode. Although the amount of O_2^- formed in this reaction is smaller than the amount of O_2^- emerging in reactions at the cathode, this should not be neglected. In particular, this reaction can also explain O_2 associated electrolyte degradation in symmetrical Li–Li cells.

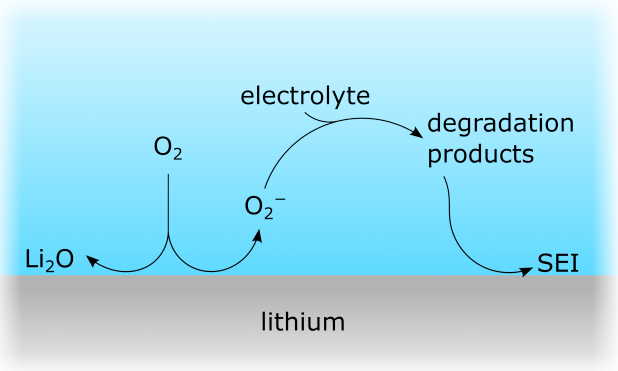

Figure 7: Scheme of possible pathways of the reaction between O_2 and the lithium electrode.

3 Results & Discussion

3.1 Understanding the Transport of Atmospheric Gases in Liquid Electrolytes for Lithium–Air Batteries (1st Publication)

The first publication of this thesis focuses on the solubility and diffusivity of O_2, N_2 and CO_2 in different electrolytes for Li–O_2 batteries. Its primary objective is to supplement the existing knowledge on the solubility of O_2 in pure solvents[71] by including data on CO_2 and N_2 solubility as well as the impact of LiTFSI as conducting salt. Gas uptake measurements were used to determine Henry's law solubility constants H^{cp} and diffusion coefficients D experimentally. In addition, the diffusion coefficients were calculated with MD simulations.

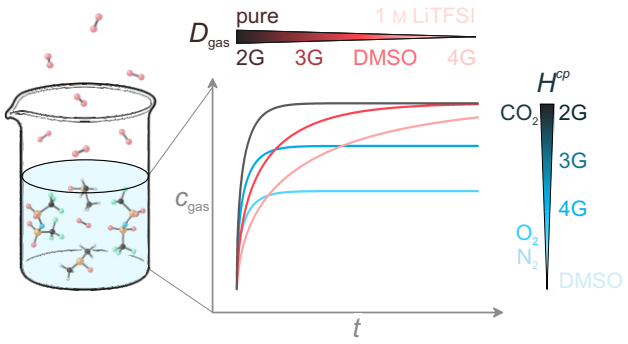

Figure 8: Graphical abstract of the first publication.

The experiments showed that the solubility of O_2 and N_2 can be described very well by the cavity model described in section 2.2.1 and that a linear relationship between $\ln L$ and σ is obtained (equation 12), which allows a prediction of the solubility from tabulated surface tension data. However, the solubility of CO_2 is significantly larger and cannot be described by the model. Furthermore, it was found that the addition of LiTFSI decreased gas solubility in ethers but increased it in DMSO. Thus, depending on the solvent, both salting-out and salting-in effects can be observed. For diffusivity, experimentally determined and simulated diffusion coefficients were compared and a good qualitative agreement was found. In general, the diffusion coefficients of the different gases were very similar and the diffusivity depended mainly on the solvent used. It was also shown that the addition of LiTFSI reduced the gas diffusivity in all cases, which can be explained by the increased viscosity. Especially at high concentrations, where CIPs are formed, the diffusivity decreased drastically.

The experiments presented in this publication were planned and conducted by the first author under the supervision of D. Schröder and J. Janek. MD simulations of the diffusion coefficients were performed by M. Murat and A. Natan. The manuscript was written by the first author and edited by all co-authors.

Reprinetd with permission from R. Haas, M. Murat, M. Weiss, J. Janek, A. Natan and D. Schröder Understanding the Transport of Atmospheric Gases in Liquid Electrolytes for Lithium–Air Batteries, *J. Electrochem. Soc.*, **2021**, *168*, 070504, DOI: 10.1149/1945-7111/ac0d66.

Journal of The Electrochemical Society, 2021 **168** 070504

Understanding the Transport of Atmospheric Gases in Liquid Electrolytes for Lithium–Air Batteries

Ronja Haas,[1,2] Michael Murat,[3,4] Manuel Weiss,[1,2] Jürgen Janek,[1,2] Amir Natan,[5,z] and Daniel Schröder[6,z]

[1]*Institute of Physical Chemistry, Justus Liebig University Giessen, 35392 Giessen, Germany*
[2]*Center for Materials Research (LaMa), Justus Liebig University Giessen, 35392 Giessen, Germany*
[3]*Department of Physical Electronics, Tel Aviv University, Tel Aviv 69978, Israel*
[4]*Soreq NRC, Yavne 81800, Israel*
[5]*The Raymond and Beverly Sackler Center for Computational Molecular and Materials Science, Tel Aviv University, Tel Aviv 69978, Israel*
[6]*Institute of Energy and Process Systems Engineering (InES), Technische Universität Braunschweig, 38106 Braunschweig, Germany*

In metal–air batteries, carbon dioxide (CO_2) and nitrogen (N_2) are, apart from oxygen (O_2), also present as dissolved species in the liquid electrolyte. These dissolved gases can strongly influence the battery performance, as they affect the discharge mechanism and the stability of the lithium metal anode. Therefore, their solubility and diffusivity are important parameters, that are rarely considered in the development of electrolytes for metal–air batteries. In this work, the diffusion coefficients (D) and Henry's law solubility constants (H^{cp}) of O_2, N_2 and CO_2 in common ether-based (diglyme (2G), triglyme (3G) and tetraglyme (4G)) and DMSO-based electrolytes are measured by means of gas uptake measurements. Additionally, the diffusion coefficients are calculated through molecular dynamics simulations. The results agree well with the experimental data. Furthermore, the influence of solvent parameters, such as surface tension and viscosity, on the solubility and the diffusivity as well as the impact of the addition of LiTFSI as conducting salt are investigated. The reported data will help to assess the impact of dissolved gases on the cell chemistry of nonaqueous lithium–air batteries, especially on the solid electrolyte interphase (SEI) at the lithium anode, and to predict diffusivity and gas solubility in other electrolytes.
 [DOI: 10.1149/1945-7111/ac0d66]

Manuscript submitted April 12, 2021; revised manuscript received May 28, 2021. Published July 1, 2021.

Supplementary material for this article is available online

Metal–air batteries are considered as future alternatives next to lithium-ion batteries because of their high energy density. Compared to other metal–air batteries with e. g. Na, Zn or Al anodes, Li–air batteries promise the highest theoretical energy density. However, their commercialization is still out of reach, since they suffer from severe chemical challenges and drawbacks:[1–5] Oxygen redox reactions have low rate capability[1] and, especially in the case of the oxygen evolution reaction (OER), very high overpotentials. High charging voltages[6] and reactive oxygen intermediates such as superoxide[7–9] and singlet oxygen[10–12] can lead to decomposition of the cathode material and the electrolyte. The lithium anode is currently also not sufficiently stable, due to dendrite formation and side reactions with the electrolyte or species dissolved therein.[13,14] Particularly the reaction of the metal anode with electrolyte may cause drying-out of full cells and fast cell failure.

The careful selection of the electrolyte is of central importance, as it has a great impact on the battery cell and its properties. For example, the discharge mechanism is determined by the Lewis basicity of the electrolyte used.[15] Many of the aforementioned problems can be addressed by adapting the electrolyte, i.e. by changing the solvent or the conducting salt or by enclosing additives (e.g. redox mediators or SEI-forming additives, etc). [13,16–23]

The current density that can be achieved during discharge also depends on the electrolyte and is determined by the concentration c_{O_2} and the diffusion coefficient D_{O_2} of oxygen. The mass transport limiting current I_{lim} can be calculated from

$$I_{lim} = nFAD_{O_2}c_{O_2}\cdot\delta^{-1} \quad [1]$$

with n as the number of transferred electrons, F as Faraday's constant, A as surface area of an ideal planar electrode and δ as thickness of the Nernst layer through which O_2 has to diffuse.[24] The concentration of oxygen is limited by its solubility in the electrolyte and can be calculated from the O_2 partial pressure p_{O_2} in the gas reservoir and Henry's law solubility constant H^{cp} using

$$c_{O_2} = H^{cp}\cdot p_{O_2} \quad [2]$$

Looking at these equations, the achievable discharge current can be maximized, e.g. to enable fast discharge, by maximizing the diffusion coefficient and Henry's law solubility constant of O_2.[25] However, cathode structure and wettability are also important parameters that influence the achievable limiting current.[26,27]

Apart from that, dissolved gases in the liquid electrolyte can diffuse to the anode and react with the lithium anode.[9,28] In Li–air batteries, O_2, N_2 and CO_2 from ambient air can be dissolved in the electrolyte. Moreover, CO_2 emerges from side reactions of the electrolyte or electrochemical decomposition of electrolyte or carbon cathode and is therefore also present in Li–O_2 batteries that are operated with pure O_2. Each of these gases reacts with lithium and thus has significant impact on the composition and stability of the solid electrolyte interphase.[13,14,29–31] In order to assess the influence of dissolved gases on the anode, their concentration, which is limited by the solubility, and mobility that is determined by the diffusivity are important parameters. Furthermore, solvated CO_2 and N_2 also influence the cathode reaction.[14,32–35] CO_2 reacts with Li_2O_2 and leads to the formation of Li_2CO_3 as discharge product, resulting in a significant increase of the overpotential during charging, hindering the intended decomposition of Li_2O_2 by redox mediators.[34–36] Therefore, the solubility and, thus, the concentration of CO_2 should be reduced as much as possible.

Some data for O_2 diffusivity and solubility are already available in literature, obtained from many different measurement methods, mostly electrochemically by cyclic voltammetry or rotating disc electrode measurements.[37–42] Unfortunately, the values show large

[z]E-mail: amirnatan@post.tau.ac.il; d.schroeder@tu-braunschweig.de

Journal of The Electrochemical Society, 2021 **168** 070504

dependence on the measurement method and are often not comparable. Moreover, solubility and diffusion coefficient of CO_2 and of N_2 are not easily measured electrochemically and are hardly known in the literature for any system that is relevant for lithium-based batteries, even though CO_2 diffusivity and solubility are also crucial for the ongoing research on Li–CO_2 or Li–O_2/CO_2 batteries.[30,43]

In this work, we used gas uptake measurements to determine the solubility and the diffusivity of O_2, of N_2 and of CO_2 in different DMSO-based and ether-based electrolytes that are commonly used in nonaqueous Li–air batteries, as well as in the pure solvents. This method facilitates measurements in pure solvent without conducting salt, as well as the determination of solubility and diffusivity of CO_2 and of N_2. We discuss how these two properties depend on the nature of the solvent and on the impact of the conducting salt. Additionally, we perform MD simulations and compare diffusion coefficients obtained from different force fields to experimental data. The obtained data will help to identify optimal electrolytes for the next generation of metal–air batteries.

Experimental

Molecular dynamics simulations.—Molecular Dynamics (MD) simulations were performed with the LAMMPS package[44] for glymes with varied molecular length, DMSO, DMSO + LiTFSI and glymes + LiTFSI at varied concentrations of LiTFSI. The diffusion coefficients of O_2, of N_2 and of CO_2 in those solvents were calculated also with the LAMMPS package. The initial structure files and LAMMPS input files were prepared with Packmol[45] and Moltemplate,[46] respectively. The OPLS-AA Force Field (FF) was used for the glymes; we used the torsion parameters given in Table IV of Anderson and Wilson,[47] in rows corresponding to the DME force field.[47] For DMSO, we have used the FF of Strader et al. and had good agreement, for some basic parameters, with both Strader et al.[48] and Vishnyakov et al.[49] For LiTFSI, we used force field parameters as given in Canongia Lopes et al.[50] and applied the suggestion by Tong et al.[51] for charge rescaling. For O_2 we checked two different force fields. Firstly, we used a force field after Arora and Sandler,[52] which we also used in previous work.[37,53] This force field has no charges on the oxygen atoms, and to check the effect of the oxygen quadrupole moment we used another force field by Vujic and Lyubartsev.[54] In this force field, the oxygen atoms have a charge of $-0.112e$ and there is also a virtual mass-less center charge of $+0.224e$. Those charges are intended to reproduce the oxygen quadrupole moment. For N_2 we also used the parameters from Vujic and Lyubartsev;[54] there is a charge on the N atoms and a virtual opposite charge in the center to reproduce the nitrogen quadrupole moment. For CO_2 we used the force field parameters from Cygan et al. in most simulations.[55] To double check our results for the CO_2 diffusion coefficient, we checked it in triglyme also with the CO_2 force field parameters from Zhang and Duan[56] and from Higashi et al.[57]

Taking realistic values for the concentration of O_2 leads to having one or less O_2 molecules in the simulation cell.[53] In previous work, we have therefore used only one O_2 molecule and did a time average of the mean squared displacement (MSD) for the diffusion coefficient. Here, we used up to 10 gas molecules inside the solvent instead. We have verified in some of the cases that this does not lead to a major difference in the calculated diffusion coefficient and helps to reduce the statistical noise as there are more gas molecules.

Our simulations start with an initial configuration constructed using the Packmol package. The system contains all the molecular species (solvent and gas molecules, with the ionic species for the simulations with salt) in a cubic box larger than the expected size of the equilibrated system. We then run a short (≈100 ps) constant volume simulation at 298 K to locally relax any high energy configurations that may have been created. This is followed by a longer (≈1 ns) constant temperature and pressure (NPT) simulation at $p = 1$ atm and 298 K for the system to reach its equilibrium density. The average density is calculated with a longer ((1–5) ns) NPT simulation. We then modify the box size slightly to fix the density at its average value. Longer (50 ns) constant volume simulations are then carried out at the average density to calculate the diffusion coefficient of the gas molecules. Evaluation of the diffusion coefficient is done using the time-averaged MSD with non-overlapping time windows, as described in Kuritz et al.[53] For the evaluation of radial distribution functions, we run constant volume simulations for 10 ns, taking snapshots of the atomic coordinates every 1 ps. This is adequate for obtaining rather smooth RDF curves for most cases. Visualization of atomic structures from the simulations were made with the Vesta[58] codes.

Chemicals.—Diglyme (diethylene glycol dimethyl ether), triglyme (triethylene glycol dimethyl ether), tetraglyme (tetraethylene glycol dimethyl ether), DMSO (dimethyl sulfoxide) and LiTFSI (lithium bis(trifluoromethanesulfonyl)imide) were purchased from Sigma-Aldrich. LiTFSI was dried at 120 °C in vacuum for 24 h. The solvents were dried over 3 Å molecular sieves. All experiments were prepared in an argon-filled glovebox (MBraun) with O_2 and H_2O content below 1 ppm.

Pressure measurement and volume determination.—All pressure measurements were carried out with a PAA-33X-V-1 pressure sensor ((0–1.2) bar, KELLER AG für Druckmesstechnik), using the software control center series 30.

The volumes of the devices for solubility and diffusivity measurements were determined using a calibrated syringe (Hamilton). First, the device was evacuated. Then, defined volumes of air were added with the syringe multiple times while the pressure was monitored.

Solubility.—Henry's law solubility constants were determined as described by Schürmann et al.[37] and Hartmann et al.[40] by gas uptake measurements. 2 mL of solvent/electrolyte were filled in a glass flask (ca. 13 mL of total volume) with a magnetic stirrer that was connected to a ball valve (Swagelok) via a KF flange. The glass cell with the ball valve and a pressure sensor were connected to a stainless steel cross fitting (Swagelok). Additionally, a gas supply and a vacuum pump were connected to the cross fitting via a needle valve (Swagelok). The solvent/electrolyte was degassed prior to the experiment. A defined amount of the respective gas was then supplied to the glass flask and the solution was stirred until the pressure was constant. All measurements were carried out at 25 °C for six different pressures. Average and standard deviation were calculated for at least three different measurements.

Diffusion coefficient.—The diffusion coefficients were determined by gas uptake measurements with a thin film cell, as previously described by Hartman et al., Hou et al. and Schürmann et al.[37,40,59] A cylindrical stainless steel container (19.8 mm in diameter, 7.77 mL) was used. It was connected to a gas reservoir (ca. 26 mL) via a ball valve (Swagelok) and to a pressure sensor directly. For each measurement, 1 mL of solvent/electrolyte was filled into the thin film cell. The container was connected to a vacuum pump and the solvent was degassed prior to the experiment. Afterwards, the gas was supplied to the gas reservoir and the device was transferred to a climate chamber (Binder) at 25 °C. Then, the ball valve between gas reservoir and thin film cell was opened and closed quickly. The pressure decay during the gas uptake was measured and the diffusion coefficient was calculated according to Hartman et al., Hou et al. and Schürmann et al.[37,40,59] In each experiment, approximately (5–10) μmol of gas were dissolved in the liquid.

For further information about the measurement setups and exemplary measurements of diffusivity and solubility, the reader is referred to the explanations by Schürmann et al. and the accompanying SI.[37]

Results and Discussion

Solubility.—Table I lists the Henry's law constants of O_2, of N_2 and of CO_2 in different solvents and the electrolytes considered

Journal of The Electrochemical Society, 2021 **168** 070504

Table I. Henry's law solubility constants of O_2, of N_2 and of CO_2 measured at 25 °C given in mmol L^{-1} bar^{-1}. The values in parentheses are those measured by Schürmann et al.,[37] which are given for comparison.

solvent	O_2	N_2	CO_2
diglyme	6.5 ± 0.2 (7.1 ± 0.3)	4.3 ± 0.2	175 ± 6
triglyme	5.8 ± 0.3 (5.0 ± 0.4)	3.5 ± 0.0	162 ± 3
tetraglyme	5.2 ± 0.4 (4.3 ± 0.2)	3.0 ± 0.1	139 ± 4
DMSO	2.7 ± 0.2	1.5 ± 0.1	133 ± 2
diglyme + 1 M LiTFSI	5.9 ± 0.2 (5.5 ± 0.1)	3.4 ± 0.1	135 ± 2
triglyme + 1 M LiTFSI	4.8 ± 0.1	3.1 ± 0.0	117 ± 1
tetraglyme + 1 M LiTFSI	4.1 ± 0.5	2.7 ± 0.1	109 ± 1
DMSO + 1 M LiTFSI	3.0 ± 0.1	1.9 ± 0.1	113 ± 2
perfluorooctane	21.3 ± 0.2	14.5 ± 0.1	84.7 ± 0.3
perfluorononane	20.8 ± 0.4	13.3 ± 0.5	80.3 ± 1.5
perfluorodecaline	18.5 ± 0.5	12.0 ± 0.6	75.7 ± 0.4

herein. As Schürmann et al. already showed, the O_2 solubility in glyme ethers and perfluorocarbons (PFCs) decreases with chain length.[37] Additionally, we measured the solubility in DMSO in this work, which is significantly lower than in ethers. For N_2, we made similar observations regarding the trend in different solvents. However, the N_2 solubility is always slightly lower than the O_2 solubility. CO_2 shows by far the highest solubility in all solvents. The concentration of CO_2 in the liquids at a given pressure even exceeds the concentration in the gas phase (approx. 40.3 mmol L^{-1} bar^{-1} at 298 K according to the ideal gas law) by a factor of 3–4. Furthermore, the solubility in DMSO is unexpectedly high; Henry's law constant for CO_2 in DMSO is almost equal to that of CO_2 in tetraglyme. The outstanding solubility of CO_2 is already known from literature and was already investigated in various organic solvents.[60,61] However, the solubility of CO_2 in PFCs, that provide excellent gas dissolving properties for most gases, is even reduced.

In order to understand the solubility of gases in liquids, many models have been established.[62,63] According to the cavity model, the uptake of a gas molecule in a liquid can in theory be divided into two steps: First, a cavity with the size of the gas molecule is created. For this, work against the surface tension σ of the liquid has to be carried out. Second, the gas molecule is inserted into the cavity, resulting in a gain of interaction energy E between solvent and the inserted molecule.[64–66] From these hypotheses, Eq. 3, in which k_B is the Boltzmann constant and T the temperature, can be derived for a spherical solute with radius r.[66] Assuming an interaction energy that is independent of the solvent, this leads to a linear relation between the logarithm of the ratio of solute concentration in the liquid c_l and in the gas phase c_g and the surface tension.

$$\ln\left(c_l \cdot c_g^{-1}\right) = -[(4\pi r^2\sigma + E)(k_B T)^{-1}] \qquad [3]$$

In Fig. 1, Eq. 3 is evaluated for the data presented in Table I. The solubilities of O_2 and N_2 follow a linear trend and are therefore well described with the cavity model. The radii obtained from the slope of the linear fit of $\ln\left(c_l \cdot c_g^{-1}\right)$ against the surface tension are 156 pm for O_2 and 164 pm for N_2, respectively. Even though the molecules are not exactly spherical, these radii are in good agreement with the values calculated from van der Waals constants.[66] However, the radius of N_2 and of O_2 is very similar in both experiment and literature and cannot explain the higher solubility of O_2. According to the model, this can be explained by the interaction energy between gas and solvent. The y-axis intercepts for both, O_2 and N_2, are positive, which means that the interactions between gas and solvents are attractive. O_2, however has a larger intercept and therefore stronger intermolecular interactions with the solvents, resulting in a slightly higher solubility. With the linear relation between the logarithm of the solubility and the surface tension, it is now possible to estimate the solubility of O_2 and N_2 in other solvents from tabulated surface tension data.

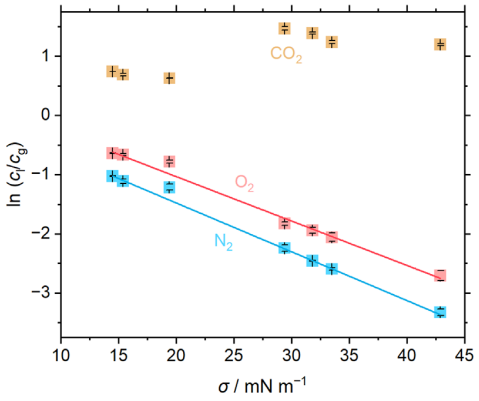

Figure 1. Logarithm of c_l/c_g of CO_2 (orange), of O_2 (red) and of N_2 (blue) as function of the surface tension of the solvent. Linear trends according to Eq. 3 are observed for O_2 and N_2, but not for CO_2. In all solvents the order of Henry's law solubility constants is $CO_2 > O_2 > N_2$.

The higher solubility of CO_2 can be ascribed to stronger solvent–gas interactions. The partially positively polarized carbon and the negatively polarized oxygen lead to stronger attractive interactions with solvent molecules, while O_2 and N_2 only form very weak interactions with the solvent. Therefore the solubility of CO_2 is even one or two orders of magnitude higher than the solubility of N_2 and O_2. The interaction energy between CO_2 and DMSO seems to be even higher than in diglyme, triglyme and tetraglyme. Due to the weak interactions between the PFCs and other molecules, including CO_2, the solubility of CO_2 in these solvents is even lower than in the ethers and DMSO. Because of the large difference in interaction energies between CO_2 and different solvents, the linear relation between $\ln\left(c_l \cdot c_g^{-1}\right)$ and σ does not hold for CO_2.[66]

From Table I it is evident that the addition of 1 M LiTFSI to the electrolyte reduces the gas solubility for most of the solvent–gas combinations. Only the solubility of O_2 and of N_2 in DMSO is increased in the electrolyte with 1 M LiTFSI.

The decrease in solubility when a salt is added can be explained by the salting out effect. Debye explained the impact of the salt on the solubility with the influence on the dielectric constant of the solvent. According to this model, an increase of the dielectric constant leads to salting in, a decrease of the dielectric constant to salting out.[67] This concept works well for the solubility of different salts, but is restricted to solutes that have a higher total molecular polarization than the solvent.[68] For solutes that have a lower total molecular polarization, like O_2 and N_2, salting in is more due to interactions between gas and ions, the so called "lyotropic salting in Refs. 68, 69." This effect is observed for large ions, which form

Journal of The Electrochemical Society, 2021 **168** 070504

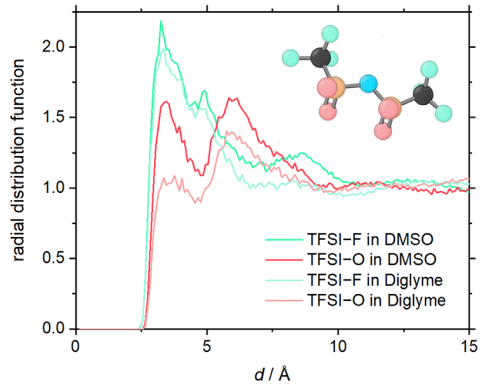

Figure 2. Radial distribution function of O_2 with fluorine (green) and oxygen (red) of the TFSI anion in 1 M solutions in diglyme and DMSO. The distance of O_2 to fluorine is similar in both solvents, but oxygen coordination is stronger in DMSO.

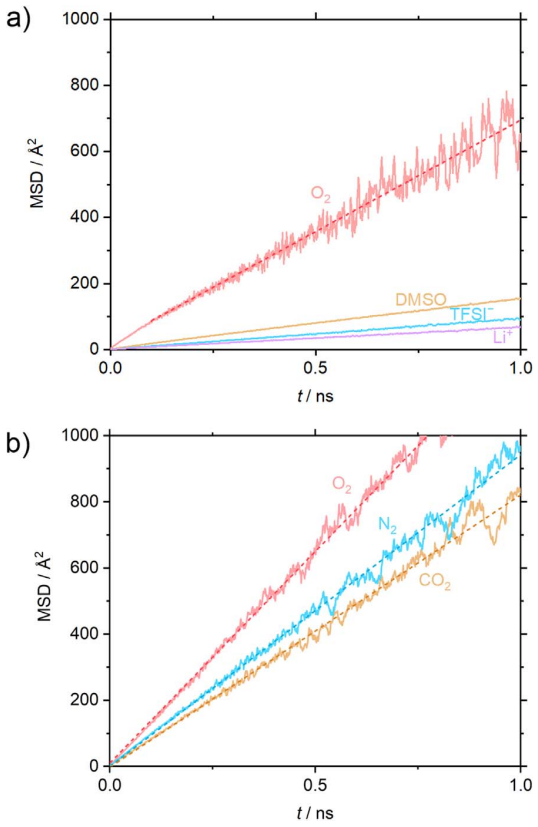

Figure 3. Mean-squared displacement (MSD) of (a) O_2 and DMSO molecules, as well as the anion and the cation in a 1 M LiTFSI solution in DMSO with dissolved O_2 and (b) O_2, N_2 and CO_2 in pure DMSO as a function of time. Diffusion constants evaluated from the slopes of the linear fits (shown as dashed lines for the dissolved gases) to these curves are listed in Table II. The total length of the simulation shown in (a) was 40 ns. Note that the higher noise in the MSD values for O_2 compared to the MSD in other species is due to the fact that the simulated system contained only one O_2 molecule, compared to 300 DMSO molecules and 25 LiTFSI molecules. The simulations shown in (b) for each gas were performed using 300 DMSO molecules and 10 gas molecules, and were run for 10 ns. The simulation for O_2 is with the neutral oxygen force field.

dispersion interactions with other solutes.[39,69] In ethers, where the gas solubility is higher, these interactions are not strong enough to further increase the solubility with LiTFSI. The same applies for CO_2 that forms much stronger interactions with the solvents, especially DMSO.

In order to demonstrate the interactions of O_2 with $TFSI^-$ ions, we calculated the radial distribution functions (RDF) from the MD simulations of O_2 in a 1 M solution of LiTFSI in DMSO (Figs. S1a and S1b available online at stacks.iop.org/JES/168/070504/mmedia) and diglyme (Figs. S1c and d). The graphs show that O_2 is coordinated by fluorine and oxygen atoms of the TFSI anion. In general, the $TFSI^-$ concentration is elevated in the surrounding of O_2 more than the concentration of the solvent. In Fig. 2, the radial distribution function of O_2 with fluorine and oxygen of $TFSI^-$ is compared for DMSO-based and diglyme-based electrolytes. The coordination of O_2 by the $TFSI^-$ fluorine is almost similar in both solvents, the coordination with the $TFSI^-$ oxygen is stronger in DMSO. This supports our observations on the impact of the salt on the gas solubility in different solvents. In DMSO, O_2 is strongly coordinated by TFSI anions, resulting in an improved solubility when LiTFSI is added.

Diffusivity.—In this part, we compare our experimental and theoretical results for the diffusion coefficient of the three gases in the pure solvents and also the solvents with 1 M of LiTFSI. Table II summarizes the results of both simulation and experiment for the diffusion coefficient of all three gases in glymes and DMSO with and without salt. For O_2 we have calculated the diffusion coefficient in the pure solvents with two FFs, the first without charges as in Schürmann et al.,[37] the second FF with charges that represent the O_2 quadrupole moment (value given in parentheses). It is evident that the difference between the two FFs is very small, with the latter leading to a slightly smaller diffusion coefficient. We continued the rest of the simulations with the neutral FF. Figure 3a shows the MSD of all the molecular species in a 1 M solution of LiTFSI in DMSO with dissolved O_2 as a function of time. In Fig. 3b we show the MSD of the three gases in DMSO as a function of time.

While there is no perfect quantitative agreement between simulation and experiment, there is an excellent qualitative agreement in the trends as shown in Fig. 4. Quantitatively, it is evident from Fig. 4 that the simulated values of the diffusion constant are roughly half of those that were measured by the experiment, but they

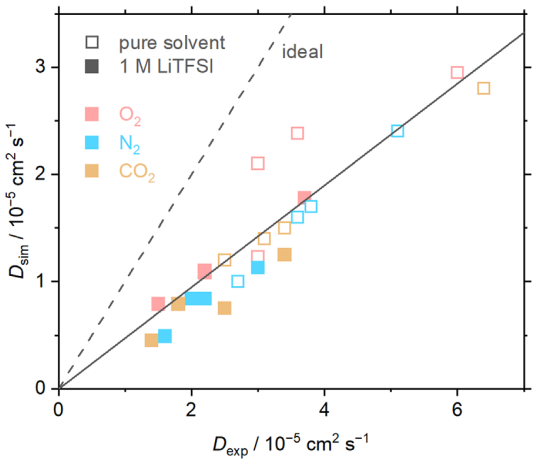

Figure 4. Correlation between diffusion coefficients obtained from MD simulation (*y*-axis) and experiment (*x*-axis). The experimentally determined diffusion coefficients are higher than the diffusion coefficients from the simulations by a factor of 2.1 ($R^2 = 0.80$). O_2 data are shown in red, N_2 is shown in blue and CO_2 is shown in orange.

Journal of The Electrochemical Society, 2021 **168** 070504

Table II. Diffusion coefficient results for all three gases, given in 10^{-5} cm^2 s^{-1}. The values in parentheses for O_2 represent the results with the charged FF.[54] For CO_2 most of the results are with the FF by Cygan et al.,[55] the values in parentheses for CO_2 in triglyme represent additional results with: (a) the FF of Zhang and Duan[56] and (b) the FF of Higashi et al.[57]—as is evident, the results are almost identical. We estimated the statistical error in the simulation diffusion coefficients to be around 10%–15%. The statistical error of the diffusion coefficients from experiments is approximately 0.5 cm^2 s^{-1}.

Solvent	O_2		N_2		CO_2	
	Simulation	Experiment	Simulation	Experiment	Simulation	Experiment
monoglyme	7.43 (6.1)	—	5.5	—	5.1	—
diglyme	2.95 (3.1)	6.0	2.4	5.1	2.8	6.4
triglyme	2.38 (2.0)	3.6	1.7	3.8	1.5 (1.2[a]; 1.4[b])	3.4
tetraglyme	1.23 (1.2)	3.0	1.0	2.7	1.2	2.5
DMSO	2.1 (1.9)	3.0	1.6	3.6	1.4	3.1
monoglyme + 1 M LiTFSI	3.2	—	2.45	—	2.28	—
diglyme + 1 M LiTFSI	1.78	3.7	1.16	3.0	1.25	3.4
triglyme + 1 M LiTFSI	1.08	2.2	0.84	2.0	0.79	1.8
tetraglyme + 1 M LiTFSI	0.79	1.5	0.49	1.6	0.45	1.4
DMSO + 1 M LiTFSI	1.1	2.2	0.84	2.2	0.75	2.5

keep exactly the same trend, this could be attributed to an insufficient description of the interactions by the force field model, such a factor is not uncommon in the literature. In both the simulation and the experiment, the diffusivity of all gases decreases with increasing length of the glyme chain. In the theoretical calculations, the diffusion coefficient of the gases in DMSO is very close to that of triglyme. In the experiment the results for DMSO are somewhere between triglyme and tetraglyme. Both the simulation and experiment show that the diffusion coefficients of all the three gases are quite close in value to one another. The simulation shows that in all solvents the diffusion coefficient of O_2 is higher than that of N_2 and of CO_2 which have similar values. Thus, the stronger interactions of the solvents with CO_2 do not seem to have any influence on the diffusion coefficient. Due to the larger solvate shell, molecules that interact more strongly with the solvent would be expected to diffuse more slowly.

The addition of 1 M LiTFSI decreases the diffusion coefficient by almost a factor of two for all gases in all solvents, this trend is evident by both the simulation and the experimental measurements and also makes sense in view of the fact that the viscosity is increased by addition of the salt. To see the impact of the salt concentration in a more detailed way, we have performed MD simulations with various LiTFSI concentrations ranging from 0.1 M to 3 M. In all simulations with the salt, 300 DMSO molecules, one O_2 molecule and the number of LiTFSI molecules indicated in Table III were added in the simulation cell. 300 DMSO molecules and 10 O_2 molecules were added to the simulation cell for the case of no salt added.

We reveal that the diffusion coefficient of O_2, as well as the self-diffusion of DMSO, $TFSI^-$ and Li^+, decrease when increasing the salt concentration. At concentrations of 2.5 M and 3 M we see a large decrease in the self-diffusion coefficients relative to the 2 M concentration, suggesting that the large molecules as well as the lithium ion become less mobile. For the diffusion coefficient of O_2 we see a decrease almost by a factor of two when moving from 2 M to 2.5 M salt concentration. In addition to a change in the diffusion coefficient, we also see an increase in the viscosity of the liquid with increasing salt concentration. The self-diffusion of DMSO was calculated to be 5.7×10^{-6} cm^2 s^{-1}. This value is not far from the experimental results of 7.3×10^{-6} cm^2 s^{-1} by Holz et al.[70] and 9.5×10^{-6} cm^2 s^{-1} by Packer et al.,[71] which were found with NMR measurements, and theoretical results of 9.5×10^{-6} cm^2 s^{-1} by Vishnyakov et al.[49] and 3.58×10^{-6} cm^2 s^{-1} by Wang and Hou.[72]

In order to explain the severe decrease of the diffusion coefficients in the 3 M electrolyte, we also calculated the RDF of Li^+ for different concentrations of LiTFSI. The RDFs at 1 M are shown in the SI for both, DMSO and diglyme. At lower TFSI concentrations, the lithium ions are coordinated mostly by oxygen atoms of the solvent, whereas TFSI ions are no closer than 5 Å. This is also illustrated in a snapshot of the simulation of 1 M LiTFSI in DMSO in Fig. 5c. Li^+ is coordinated by four DMSO molecules, which is consistent with literature on the coordination number of Li^+ in DMSO.[73,74] In Fig. 5, the RDF of Li^+ is shown with (a) oxygen of $TFSI^-$ and (b) Li^+ for different concentrations of LiTFSI in DMSO. In Fig. 5a, two peaks at 2.4 Å and 4.7 Å emerge for the 2.5 M and 3 M solution, indicating that Li^+ is also coordinated by $TFSI^-$ and contact ion pairs are formed at concentrations above 2 M. The significantly lower diffusivity of Li^+, $TFSI^-$ and DMSO in the 2.5 M and 3 M solution can therefore be attributed to the formation of contact ion pairs, which takes place at concentrations above approximately 2.3 M and leads to a significant reduction of the mobility of the ions and the solvent.[75,76] This also leads to an increase of the viscosity and hence to a reduction of gas diffusivity. Additionally, we observed that in the 2.5 M and 3 M solution, a Li^+ peak appears at 3.0 Å in the Li^+ RDF. As shown in a snapshot of the simulation af the 3 M solution in Fig. 5d, two lithium ions share up to three oxygen atoms of DMSO or $TFSI^-$.

Conclusions

Electrolytes for Li–air batteries are often selected according to their ionic conductivity and stability towards anode, reactive oxygen intermediates and electrochemical decomposition. However, transport properties of dissolved gases are often overlooked, even though they play a major role in limiting current density during discharge (O_2) and stability towards the anode (O_2, N_2, and CO_2) and should therefore be considered in the selection of the electrolyte. Therefore, we have determined solubility and diffusivity of these gases in electrolytes and solvents that are commonly used in Li–air batteries by means of MD simulations and gas uptake measurements in this work.

For the diffusion coefficients, we found a good qualitative agreement between experimental data and simulation results. This finding indicates that the results of both methods are conclusive. In addition, measurements of CO_2 and of N_2 could be easily performed, and pure solvents without conducting salt could be used, which is not possible with usual electrochemical measurement methods. This benefit makes our method and the obtained results particularly interesting for Li–CO_2 batteries.

Since the diffusion coefficient was found to be almost independent of the dissolved gas, the solubility is decisive for estimating the

Journal of The Electrochemical Society, 2021 **168** 070504

Table III. Effect of LiTFSI concentration in DMSO on density, viscosity and diffusion coefficients. Unless indicated otherwise, simulation length for all cases is (1–5) 10^7 fs. At 2.5 M and 3 M LiTFSI, the viscosity is significantly increased and all diffusion coefficients are decreased as a result. (*)This system is run for 2×10^8 fs, but it still seems to be too short for calculating the diffusion coefficients reliably. The range of *D* values are from simulations of different length. We estimated the statistical error in the simulated diffusion constant to be around 15% for the O_2 and around 5% for all the rest (DMSO, $TFSI^-$, and Li^+).

c_{LiTFSI}, Target/Actual/M	No. of LiTFSI molecules	Density/g cm^{-3}	Viscosity/cP	Diffusion coefficient/10^{-5} cm^2 s^{-1}			
				O_2	DMSO	$TFSI^-$	Li^+
0.0/0.0	0	1.086	1.7	2.1	0.57	—	—
0.1/0.136	3	1.100	1.7	2.2	0.54	0.32	0.23
0.5/0.52	12	1.155	1.9	1.9	0.38	0.25	0.14
1.0/0.99	25	1.217	2.3	1.1	0.25	0.14	0.11
2.0/1.84	54	1.330	3.1	0.76	0.061	0.047	0.037
2.5/2.62	90	1.435	4.0	0.47	0.0096	0.010	0.0088
3.0/3.12(*)	120	1.503	4.6	0.28–0.36	0.0043–0.0046	0.0041–0.0050	0.0039–0.0043

Journal of The Electrochemical Society, 2021 **168** 070504

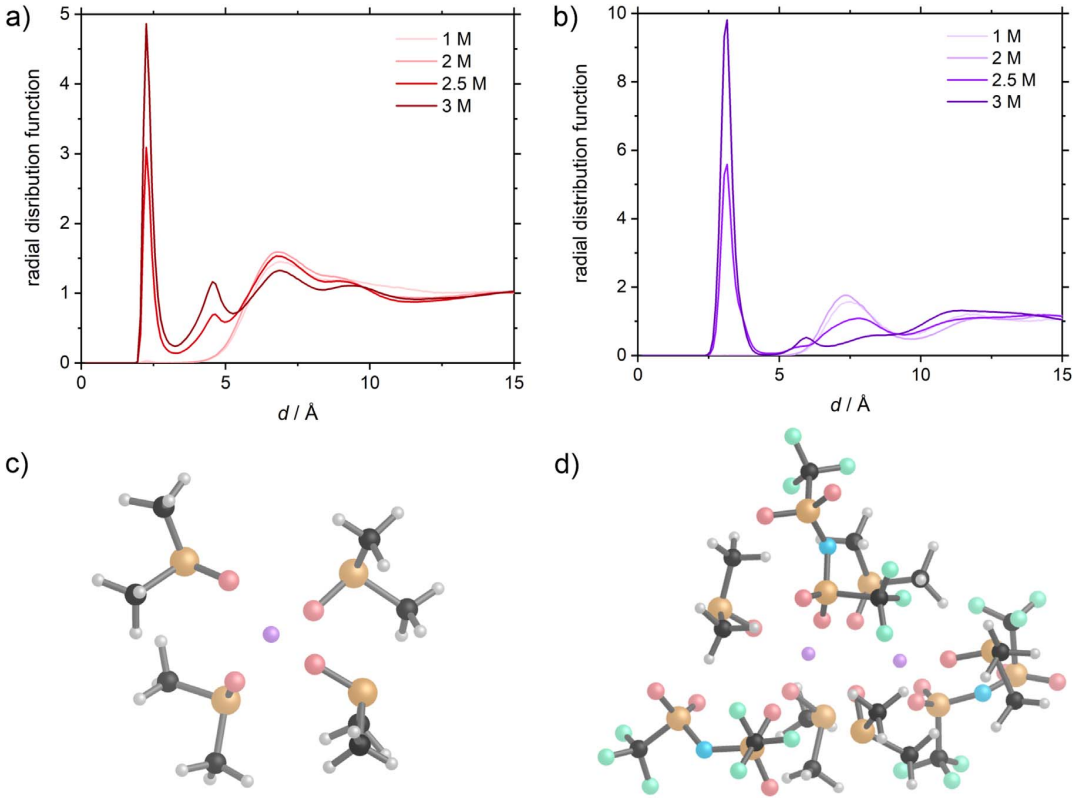

Figure 5. RDF of Li^+ with (a) O of $TFSI^-$ and (b) Li^+ at different LiTFSI concentrations in DMSO. The enrichment of $TFSI^-$ closer than 3 Å to Li^+ in 2.5 M and 3 M solutions indicates the formation of contact ion pairs. (c), (d) Snapshots from MD simulations of the Li^+ surrounding in (c) 1 M and (d) 3 M LiTFSI in DMSO. Carbon is shown in black, hydrogen in light grey, oxygen in red, nitrogen in blue, fluorine in green, sulfur in yellow and lithium in purple. In the 1 M solution (c), Li^+ is surrounded by four DMSO molecules. In the 3 M solution (d) Li^+ is surrounded by DMSO and $TFSI^-$ and close to a second Li^+.

influence of the different gases on anode stability and cathode kinetics. Unfortunately, CO_2 that leads to the formation of unwanted Li_2CO_3 as discharge product, has by far the highest solubility in all tested solvents and electrolyte. However, in contrast to O_2 and N_2, the solubility of CO_2 did not follow the expected trend that gas solubility decreases with increasing surface tension of the solvent. Instead, the solubility of CO_2 was lowest in PFCs, which are very nonpolar and have low surface tensions. Due to good O_2 solubility and lowest CO_2 solubility, PFCs are promising for use in Li–air batteries.

In addition, the oxygen solubility in DMSO can be increased by adding LiTFSI, while the CO_2 solubility is reduced as a result. Since the type of conducting salt determines the impact on the O_2 solubility, the ratio of O_2 to CO_2 can also be changed by the choice of conducting salt. Since PFCs have desirable properties in this regard, the effect of LiTFSI could partially be attributed to the fluorinated methyl groups. Therefore, salts with longer fluorinated alkyl groups could further increase O_2 solubility while simultaneously decreasing CO_2 solubility. However, the concentration of the conducting salt should not be too high since contact ion pairs reduce the conductivity of the electrolyte and slows down O_2 diffusion.

Overall, the results obtained here can help in designing tailored electrolytes for Li–air batteries. For batteries where maximized discharge current density is required, the O_2 solubility and diffusivity should be as high as possible. However, which gases in the electrolyte lead to a more stable SEI has not yet been finally determined. A hybrid cell setup with different anolyte and catholyte may be the solution to achieve ideal gas solubility and diffusivity for both electrodes.

Acknowledgments

We thank Yair Ein-Eli and Adrian Schürmann for fruitful discussions. The authors acknowledge financial support by the Federal Ministry for Education and Research within the ELONGATE project (03XP0248) and by the DFG via the GRK (Research Training Group) 2204 “Substitute Materials for sustainable Energy Technologies”; support for the ELONGATE project on the Israeli side was given by the ministry of science and technology, grant number 3-16021. AN would like to also thank the Planing & Budgeting Committee of the Council of High Education and the PrimeMinister Office of Israel, in the framework of the INREP project.

ORCID

Jürgen Janek https://orcid.org/0000-0002-9221-4756
Amir Natan https://orcid.org/0000-0003-4517-5667
Daniel Schröder https://orcid.org/0000-0002-2198-0218

References

1. P. G. Bruce, S. A. Freunberger, L. J. Hardwick, and J. M. Tarascon, *Nat. Mater.*, **11**, 19 (2012).
2. G. Girishkumar, B. McCloskey, A. C. Luntz, S. Swanson, and W. Wilcke, *J. Phys. Chem. Lett.*, **1**, 2193 (2010).
3. J. Christensen, P. Albertus, R. S. Sanchez-Carrera, T. Lohmann, B. Kozinsky, R. Liedtke, J. Ahmed, and A. Kojic, *J. Electrochem. Soc.*, **159**, R1 (2011).
4. N. Feng, P. He, and H. Zhou, *Adv. Energy Mater.*, **6**, 1502303 (2016).
5. K. M. Abraham and Z. Jiang, *J. Electrochem. Soc.*, **143**, 1 (1996).
6. M. M. Ottakam Thotiyl, S. A. Freunberger, Z. Peng, and P. G. Bruce, *J. Am. Chem. Soc.*, **135**, 494 (2013).
7. V. S. Bryantsev, V. Giordani, W. Walker, M. Blanco, S. Zecevic, K. Sasaki, J. Uddin, D. Addison, and G. V. Chase, *J. Phys. Chem. A*, **115**, 12399 (2011).

8. S. A. Freunberger, Y. Chen, N. E. Drewett, L. J. Hardwick, F. Bardé, and P. G. Bruce, *Angew. Chemie - Int. Ed.*, **50**, 8609 (2011).
9. X. Yao, Q. Dong, Q. Cheng, and D. Wang, *Angew. Chemie*, **128**, 11514 (2016).
10. N. Mahne et al., *Nat. Energy*, **2**, 17036 (2017).
11. J. Wandt, P. Jakes, J. Granwehr, H. A. Gasteiger, and R. A. Eichel, *Angew. Chemie - Int. Ed.*, **55**, 6892 (2016).
12. N. Mahne, S. E. Renfrew, B. D. McCloskey, and S. A. Freunberger, *Angew. Chemie*, **130**, 5627 (2018).
13. X. Bi, K. Amine, and J. Lu, *J. Mater. Chem. A*, **8**, 3563 (2020).
14. K. Chen, D.-Y. Yang, G. Huang, and X.-B. Zhang, *Acc. Chem. Res.*, **54**, 632 (2021).
15. Z. Peng, S. A. Freunberger, L. J. Hardwick, Y. Chen, V. Giordani, F. Bardé, P. Novák, D. Graham, J. M. Tarascon, and P. G. Bruce, *Angew. Chemie - Int. Ed.*, **50**, 6351 (2011).
16. M. Balaish, A. Kraytsberg, and Y. Ein-Eli, *Phys. Chem. Chem. Phys.*, **16**, 2801 (2014).
17. C. O. Laoire, S. Mukerjee, K. M. Abraham, E. J. Plichta, and M. A. Hendrickson, *J. Phys. Chem. C*, **114**, 9178 (2010).
18. G. M. Veith, J. Nanda, L. H. Delmau, and N. J. Dudney, *J. Phys. Chem. Lett.*, **3**, 1242 (2012).
19. Y. Chen, S. A. Freunberger, Z. Peng, O. Fontaine, and P. G. Bruce, *Nat. Chem.*, **5**, 489 (2013).
20. B. J. Bergner, A. Schürmann, K. Peppler, A. Garsuch, and J. Janek, *J. Am. Chem. Soc.*, **136**, 15054 (2014).
21. J. B. Park, S. H. Lee, H. G. Jung, D. Aurbach, and Y. K. Sun, *Adv. Mater.*, **30**, 1704162 (2018).
22. Y. K. Petit, C. Leypold, N. Mahne, E. Mourad, L. Schafzahl, C. Slugovc, S. M. Borisov, and S. A. Freunberger, *Angew. Chemie*, **131**, 6605 (2019).
23. W. Xu, J. Xiao, D. Wang, J. Zhang, and J.-G. Zhang, *J. Electrochem. Soc.*, **157**, A219 (2010).
24. A. J. Bard and L. R. Faulkner, *Electrochemical Methods : Fundamentals and Applications* (Wiley, New York) 833 (2001).
25. J. Read, K. Mutolo, M. Ervin, W. Behl, J. Wolfenstine, A. Driedger, and D. Foster, *J. Electrochem. Soc.*, **150**, A1351 (2003).
26. C. Xia, C. L. Bender, B. Bergner, K. Peppler, and J. Janek, *Electrochem. Commun.*, **26**, 93 (2013).
27. I. Bardenhagen, M. Fenske, D. Fenske, A. Wittstock, and M. Bäumer, *J. Power Sources*, **299**, 162 (2015).
28. H. Lee, D. J. Lee, J. N. Lee, J. Song, Y. Lee, M. H. Ryou, J. K. Park, and Y. M. Lee, *Electrochim. Acta*, **123**, 419 (2014).
29. E. Wang, S. Dey, T. Liu, S. Menkin, and C. P. Grey, *ACS Energy Lett.*, **5**, 1088 (2020).
30. F. Qiu, S. Ren, X. Mu, Y. Liu, X. Zhang, P. He, and H. Zhou, *Energy Storage Mater.*, **26**, 443 (2020).
31. K. Chen, G. Huang, J. L. Ma, J. Wang, D. Y. Yang, X. Y. Yang, Y. Yu, and X. B. Zhang, *Angew. Chemie - Int. Ed.*, **59**, 16661 (2020).
32. J. L. Ma, D. Bao, M. M. Shi, J. M. Yan, and X. B. Zhang, *Chem*, **2**, 525 (2017).
33. Y. S. Mekonnen, K. B. Knudsen, J. S. G. Myrdal, R. Younesi, J. Højberg, J. Hjelm, P. Norby, and T. Vegge, *J. Chem. Phys.*, **140**, 121101 (2014).
34. H. K. Lim, H. D. Lim, K. Y. Park, D. H. Seo, H. Gwon, J. Hong, W. A. Goddard, H. Kim, and K. Kang, *J. Am. Chem. Soc.*, **135**, 9733 (2013).
35. S. R. Gowda, A. Brunet, G. M. Wallraff, and B. D. McCloskey, *J. Phys. Chem. Lett.*, **4**, 276 (2013).
36. C. Ling, R. Zhang, K. Takechi, and F. Mizuno, *J. Phys. Chem. C*, **118**, 26591 (2014).
37. A. Schürmann, R. Haas, M. Murat, N. Kuritz, M. Balaish, Y. Ein-Eli, J. Janek, A. Natan, and D. Schröder, *J. Electrochem. Soc.*, **165**, A3095 (2018).
38. F. S. Gittleson, R. E. Jones, D. K. Ward, and M. E. Foster, *Energy Environ. Sci.*, **10**, 1167 (2017).
39. J. Lindberg, B. Endrődi, G. Åvall, P. Johansson, A. Cornell, and G. Lindbergh, *J. Phys. Chem. C*, **122**, 1913 (2018).
40. P. Hartmann, D. Grübl, H. Sommer, J. Janek, W. G. Bessler, and P. Adelhelm, *J. Phys. Chem. C*, **118**, 1461 (2014).
41. J. Herranz, A. Garsuch, and H. A. Gasteiger, *J. Phys. Chem. C*, **116**, 19084 (2012).
42. M. Khodayari, P. Reinsberg, A.-E.-A. A. Abd-El-Latif, C. Merdon, J. Fuhrmann, and H. Baltruschat, *ChemPhysChem*, **17**, 1647 (2016).
43. K. Takechi, T. Shiga, and T. Asaoka, *Chem. Commun.*, **47**, 3463 (2011).
44. S. Plimpton, *J. Comput. Phys.*, **117**, 1 (1995).
45. L. Martínez, R. Andrade, E. G. Birgin, and J. M. Martínez, *J. Comput. Chem.*, **30**, 2157 (2009).
46. A. I. Jewett et al., *J. Mol. Biol.*, **433**, 166841 (2021).
47. P. M. Anderson and M. R. Wilson, *Mol. Phys.*, **103**, 89 (2005).
48. M. L. Strader and S. E. Feller, *J. Phys. Chem. A*, **106**, 1074 (2002).
49. A. Vishnyakov, A. P. Lyubartsev, and A. Laaksonen, *J. Phys. Chem. A*, **105**, 1702 (2001).
50. J. N. Canongia Lopes and A. A. H. Pádua, *J. Phys. Chem. B*, **108**, 16893 (2004).
51. J. Tong, S. Wu, N. von Solms, X. Liang, F. Huo, Q. Zhou, H. He, and S. Zhang, *Front. Chem.*, **7**, 1 (2020).
52. G. Arora and S. I. Sandler, *Langmuir*, **22**, 4620 (2006).
53. N. Kuritz, M. Murat, M. Balaish, Y. Ein-Eli, and A. Natan, *J. Phys. Chem. B*, **120**, 3370 (2016).
54. B. Vujić and A. P. Lyubartsev, *Model. Simul. Mater. Sci. Eng.*, **24**, 045002 (2016).
55. R. T. Cygan, V. N. Romanov, and E. M. Myshakin, *J. Phys. Chem. C*, **116**, 13079 (2012).
56. Z. Zhang and Z. Duan, *J. Chem. Phys.*, **122**, 214507 (2005).
57. H. Higashi, Y. Iwai, H. Uchida, and Y. Arai, *J. Supercrit. Fluids*, **13**, 93 (1998).
58. K. Momma and F. Izumi, *J. Appl. Crystallogr.*, **44**, 1272 (2011).
59. Y. Hou and R. E. Baltus, *Ind. Eng. Chem. Res.*, **46**, 8166 (2007).
60. J. D. Wadhawan, P. J. Welford, E. Maisonhaute, V. Climent, N. S. Lawrence, R. G. Compton, H. B. Mcpeak, and C. E. W. Hahn, *J. Phys. Chem. B*, **105**, 10659 (2001).
61. M. Anouti, Y. R. Dougassa, C. Tessier, L. El Ouatani, and J. Jacquemin, *J. Chem. Thermodyn.*, **50**, 71 (2012).
62. R. Battino and H. L. Clever, *Chem. Rev.*, **66**, 395 (1966).
63. R. A. Pierotti, *Chem. Rev.*, **76**, 717 (1975).
64. H. Reiss, H. L. Frisch, and J. L. Lebowitz, *J. Chem. Phys.*, **31**, 369 (1959).
65. H. Reiss, H. L. Frisch, E. Helfand, and J. L. Lebowitz, *J. Chem. Phys.*, **32**, 119 (1960).
66. H. H. Uhlig, *J. Phys. Chem.*, **41**, 1215 (1937).
67. P. Debye, *Zeitschrift für Phys. Chemie*, **130U**, 56 (1927).
68. J. O. Bockris and H. Egan, *Trans. Faraday Soc.*, **44**, 151 (1948).
69. J. O. Bockris, J. Bowler-Reed, and J. A. Kitchener, *Trans. Faraday Soc.*, **47**, 184 (1951).
70. M. Holz, S. R. Heil, and A. Sacco, *Phys. Chem. Chem. Phys.*, **2**, 4740 (2000).
71. K. J. Packer and D. J. Tomlinson, *Trans. Faraday Soc.*, **67**, 1302 (1971).
72. J. Wang and T. Hou, *J. Comput. Chem.*, **32**, 3505 (2011).
73. G. Leverick, R. Tatara, S. Feng, E. Crabb, A. France-Lanord, M. Tułodziecki, J. Lopez, R. M. Stephens, J. C. Grossman, and Y. Shao-Horn, *J. Phys. Chem. C*, **124**, 4953 (2020).
74. E. Crabb, A. France-Lanord, G. Leverick, R. Stephens, Y. Shao-Horn, and J. C. Grossman, *J. Chem. Theory Comput.*, **16**, 7255 (2020).
75. A. Khetan, H. R. Arjmandi, V. Pande, H. Pitsch, and V. Viswanathan, *J. Phys. Chem. C*, **122**, 8094 (2018).
76. L. Wang, K. Uosaki, and H. Noguchi, *J. Phys. Chem. C*, **124**, 12381 (2020).

3.2 The Influence of Oxygen Dissolved in the Liquid Electrolyte on Lithium Metal Anodes (2nd Publication)

The aim of the second publication of this thesis was to get a better understanding of the influence of O_2 dissolved in the electrolyte on the lithium electrode. Since the previous literature on the subject could not come to a clear conclusion, it should also be understood which additional factors have to be taken into account and why different studies come to contradictory results.

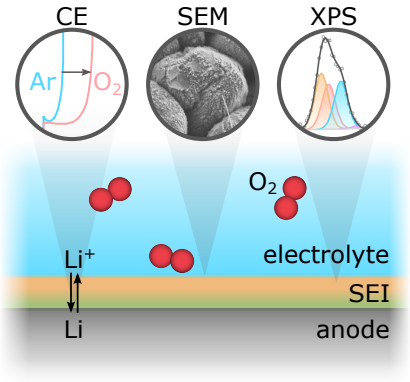

Figure 9: Graphical abstract of the second publication.

In electrochemical experiments, the plating and stripping of lithium on copper in various electrolytes was investigated. It was shown that the CE in O_2-containing electrolytes was significantly improved compared to O_2-free electrolytes. However, an even better result could be achieved with CO_2 dissolved in the electrolyte. Furthermore, SEM and XPS experiments showed that in O_2-containing electrolyte less conducting salt decomposes at the lithium electrode and a more homogeneous SEI is formed.

In addition, the SEI of lithium plated on copper was compared with the SEI on commercially available lithium foil, which is covered with an NPL. In XP spectra, significantly more fragments of the conducting salt could be detected on the commercial lithium foil, indicating increased degradation. In O_2-containing electrolytes the proportion of these degradation products was even higher. Thus, an opposite behavior to the lithium plated on copper can be observed. This difference may also explain the discrepancy between different publications on the influence of O_2 on the lithium electrode.

The experiments presented in this publication were designed by the first author under the supervision of J. Janek. All experiments were performed by the first author. The manuscript was written by the first author and edited by J. Janek.

Reprinetd with permission from R. Haas and J. Janek The Influence of Oxygen Dissolved in the Liquid Electrolyte on Lithium Metal Anodes, *J. Electrochem. Soc.*, **2022** *169*, 110527, DOI: 10.1149/1945-7111/ac9d6b.

Journal of The Electrochemical Society, 2022 **169** 110527

The Influence of Oxygen Dissolved in the Liquid Electrolyte on Lithium Metal Anodes

Ronja Haas[1,2] **and Jürgen Janek**[1,2,z]

[1]*Institute of Physical Chemistry, Justus-Liebig University Giessen, 35392 Giessen, Germany*
[2]*Center for Materials Research (LaMa), Justus-Liebig University Giessen, 35392 Giessen, Germany*

Due to the need for high energy density storage, Li–O_2 batteries and Li metal anodes (LMA) are in the focus of research. As safe operation of the LMA is yet not possible, more knowledge about factors influencing the stability of the solid electrolyte interphase (SEI) is necessary to utilize the LMA. Especially concerning the influence of O_2 dissolved in the electrolyte, there are still many unanswered questions, and there are conflicting opinions reported. In this work, plating/stripping experiments are used to show that the Coulomb efficiency is increased by dissolving O_2 in the electrolyte. SEM and XPS analysis of the SEI shows that reaction of the conducting salt with Li metal is the cause of the poor reversibility of the LMA in cells without O_2. The improved stability in the presence of O_2 can be attributed to a protective Li_2O and Li_2CO_3 rich SEI that prevents degradation. In addition, the SEI on freshly deposited Li is compared to that on a commercial Li foil. The reactivity of the native passivation layer formed on the Li foil during storage differs significantly from that of plated Li regarding the influence of O_2, which can explain the different results and conclusions in literature.

 [DOI: 10.1149/1945-7111/ac9d6b]

Manuscript submitted September 12, 2022; revised manuscript received October 19, 2022. Published November 16, 2022. *This paper is part of the JES Focus Issue on Selected Papers from IMLB 2022.*

Supplementary material for this article is available online

Due to the increasing interest in high energy density batteries, it is necessary to replace graphite anodes with Li metal to achieve the highest possible specific capacity ($Q_{theo} = 3860\ mAh\ g^{-1}$).[1] Especially Li–$O_2$ batteries promise outstanding energy densities ($Q_{theo} = 3458\ Wh\ kg^{-1}$).[2,3] However, it is challenging to produce Li metal electrodes with satisfactory stability. Due to the high reactivity of Li metal, side reactions with the electrolyte occur and a solid electrolyte interphase (SEI) is formed. Unfortunately, the SEI often cannot completely prevent side reactions of the Li metal electrode, resulting in constant Li loss and electrolyte degradation, even though many attempts are made to modify the SEI with electrolyte additives to prevent detrimental side reactions.[4]

Furthermore, in Li–O_2 batteries, O_2 is dissolved in the electrolyte and highly reactive intermediates such as superoxide (O_2^-)[5,6] and singlet oxygen ($^1O_2$)[7–10] are formed during cycling. This poses an additional threat to the stability of all cell components and the increased degradation of cathode,[11,12] solvent[13,14] and conducting salt[15,16] in the presence of O_2 were reported. Since O_2 can also diffuse to the anode and react with Li, it is often assumed that Li metal anodes in Li–O_2 batteries must be specifically protected against reactions with O_2 (e.g. by solid electrolytes, membranes, etc.).[17–19] However, the true influence of dissolved O_2 has not yet been conclusively clarified in literature.[20]

Although the influence of O_2 on the SEI has already been discussed in several articles, it is still unclear whether O_2 dissolved in the electrolyte improves or worsens the stability of the Li metal electrode, as various groups come to different conclusions on this subject: Some authors state that dissolved O_2 decreases the extent of side reactions of the electrolyte with the Li metal electrode,[21–23] while others believe that the extent of side reactions with the electrode are increased when O_2 is present.[24–26] Unfortunately, there have only been few attempts to explain the different results in the literature. In a review by Yao et al., it was suggested that dependence of the Coulomb efficiency (CE) on the O_2 concentration available at the Li metal electrode[22] could be a possible origin of converse findings.[20] However, in the article cited in the review, an improvement of the CE by O_2 was shown in each case.[22] Hence, this explanation does not cover results which indicate that dissolved O_2 enhances anode decomposition and Li loss. Therefore, the question of whether dissolved O_2 has a positive or negative effect on the Li metal electrode and why different groups arrive at different results remains unanswered.

In this study, we want to elucidate the influence of dissolved O_2 on the Li metal electrode stability. Plating/stripping of Li on Cu electrodes was used to evaluate the CE. The experiments were carried out under Ar, O_2 and CO_2 atmosphere, in order to compare the performance with dissolved O_2 to a reference (Ar) and a system where electrode protection by a gas that is known to work successfully (CO_2).[27] Additionally, the SEI formed in different environments was investigated ex situ, using scanning electron microscopy (SEM) and X-ray photoelectron spectroscopy (XPS). Thereby, we found that dissolved O_2 increases the CE of the Li metal electrode and decreases the extent of reductive decomposition of lithium bis(trifluoromethanesulfonyl)imide (LiTFSI). Furthermore, the SEI formed on freshly plated Li was compared to the SEI on commercial Li foil. We show that the reactivity of the native passivation layer (NPL) formed on Li metal differs from Li without NPL. Finally, we provide an explanation for the differences in literature concerning the influence of dissolved O_2 on Li metal electrodes.

Results and Discussion

Plating/stripping experiments.—To evaluate the stability of Li metal in contact with the electrolyte, Li was galvanostatically plated/stripped on Cu foil in different gas atmospheres. In Fig. 1a, 1 mAh of Li was plated in 1 M LiTFSI in tetraglyme, followed by 20 plating/stripping cycles of 0.1 mAh and complete stripping thereafter. A characteristic single plating/stripping cycle in the same electrolyte is shown in Fig. 1b. At least five different measurements were made for each gas and the capacity range of the stripping for each gas is shown in the respective shaded color.

In both experiments, the cells cycled in Ar (blue) showed the lowest CE; on average only 37%. For the cell cycled in O_2 atmosphere (red), the CE was significantly higher with an average of 77%. These CE are comparable to values measured by Wang et al.[23] However, Wang et al. observed an increased overpotential in the cells with O_2[23] which was not reproduced in our cells. On the contrary, in our experiments the overpotential of the cells cycled in O_2 was even lower than for Ar. Possibly, a higher water content in

[z]E-mail: juergen.janek@phys.chemie.uni-giessen.de

Journal of The Electrochemical Society, 2022 **169** 110527

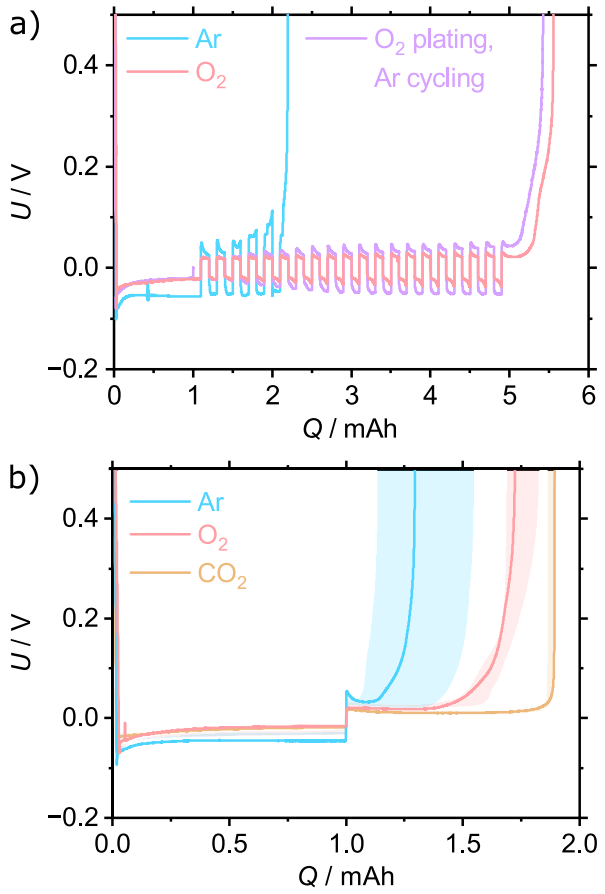

Figure 1. Plating/stripping experiments of Li–Cu cells. (a) 20 cycles à 0.1 mAh after 1 mAh plating; (b) Single plating/stripping cycle. Results for Ar are shown in blue, O_2 is shown in red and CO_2 in orange.

the electrolyte is the reason for the higher overpotential in the cells from Wang et al.[23]

Even when only the first plating step was carried out under O_2 atmosphere and the subsequent cycling took place under Ar atmosphere, the reversibility of the Li electrode was significantly improved (Fig. 1a, purple). The CE over 20 cycles was 74% and thus only slightly lower than in the cells with constant O_2 atmosphere. However, the overpotential of cells cycled in Ar increased during cycling. Nevertheless, Li electrode stability was significantly improved by O_2 exposure during the initial plating step. The success of this formation step suggests that the improved CE is caused by a more stable and protective SEI, which can be formed already during the first Li plating. This might also be relevant for the formation cycle of batteries without gas reservoir e.g. lithium metal batteries (LMB), especially with anode free cell architectures.[28]

When the plating/stripping was carried out under CO_2 atmosphere, the CE of the cells cycled in O_2 atmosphere was even surpassed (90%). Additionally, the overpotential was significantly lower in these cells. This is in line with previous results, too.[27] Also with CO_2, an initial formation step could significantly increase the CE of the Li metal electrode (Fig. S1). The performance was even as good as with cells that were constantly cycled under CO_2. It has to be noted that the solubility of CO_2 in the electrolyte is higher than the O_2 solubility by a factor of more than 25, resulting CO_2 concentrations increased by the same factor ($c(O_2) = 4.1$ mmol L^{-1}, $c(CO_2) = 109$ mmol L^{-1}).[29] However, when the partial pressure of CO_2 was reduced to 40 mbar to achieve a similar gas concentration as in cells with 1 bar O_2, the CE was lower than in

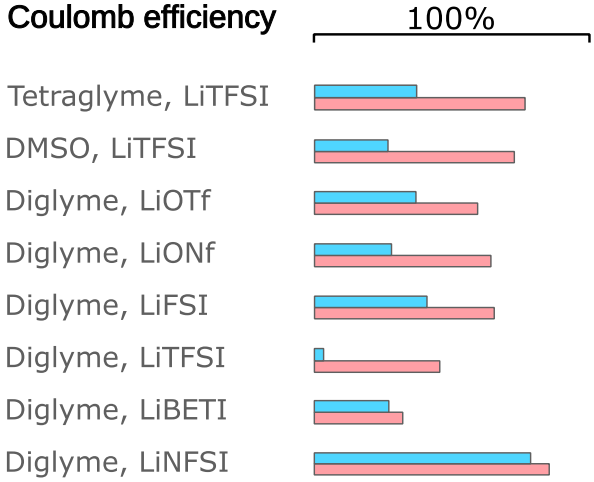

Figure 2. Coulomb efficiencies of a single plating/stripping cycle in various electrolytes. Results for Ar are shown in blue, O_2 is shown in red.

cells with 1 bar CO_2 pressure, but still higher than in cells with O_2 (Fig. S2).

We also repeated the experiments with varied solvents and conducting salts in order to confirm our results (Fig. 2). The CE was calculated from a single plating/stripping cycle of 1 mAh. Overall, the CE was very dependent on solvents and conducting salt and varied between 4% and 79% in the case without O_2. However, the cells with O_2 performed better in all tested electrolytes (32%–85%). Therefore, we assume that different electrolytes used in various studies are not the reason for disparate results concerning the influence of dissolved O_2.[21–26,30]

We also determined Henry's law solubility constants for these electrolytes (Table SI), but found no correlation to the CE from plating/stripping experiments. Hence, the O_2 concentration in the electrolyte does not seem to be the factor that determines the CE in cells with O_2. Overall, we confirm that the CE is improved by dissolving O_2 in the liquid electrolyte.[21–23]

SEI characterization.—SEM images of Li plated in different gas atmospheres are shown in Fig. 3. On the samples from Ar (a) and O_2 (b) atmosphere, a layer covering the Li chunks is visible, which is thicker in the sample from Ar atmosphere. On the CO_2 sample (c), however, almost no interphase layer is apparent, which indicates a very thin SEI. The thick SEI formed in Ar atmosphere could result in an increased resistance, which explains the higher overpotential observed in plating/stripping experiments. Also from photos of the plated Li (inserts in Fig. 3) the same trend is evident: The Li plating in CO_2 atmosphere was most homogeneous. In O_2, Li plating seems to be preferred in the center of the Cu electrode. In the Ar sample however, the Li is discolored, which indicates side reactions.

For further analysis of the SEI, we conducted XPS measurements of the Li plated in different gas atmospheres (Fig. 4; spectra after one sputter step for cleaning). Exact peak positions and assignments are given in Table SII; peak positions are in line with previous reports.[31,32]

In S 2p and F 1s spectra of samples from Ar and O_2 atmosphere, fragments of $TFSI^-$ can be seen, indicating decomposition of the conducting salt. During the reductive degradation of LiTFSI, LiTf and Li_2NTf are initially formed as intermediates, which subsequently react to form LiF, Li_2O, Li_2S, Li_3N and Li_2SO_3.[33,34] Comparison with spectra of LiTFSI powder confirms that the fragments are products of degradation and not X-ray or sputter damage (Fig. S3). Comparing the intensity or fractions of S 2p and F 1s components clarifies that significantly more $TFSI^-$ degradation takes place in Ar atmosphere than in O_2 atmosphere which is in line

Journal of The Electrochemical Society, 2022 **169** 110527

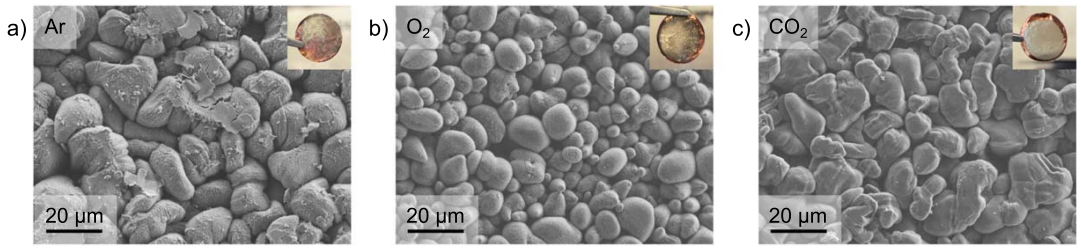

Figure 3. SEM images of Li plated on Cu in (a) Ar, (b) O_2 and (c) CO_2 atmosphere.

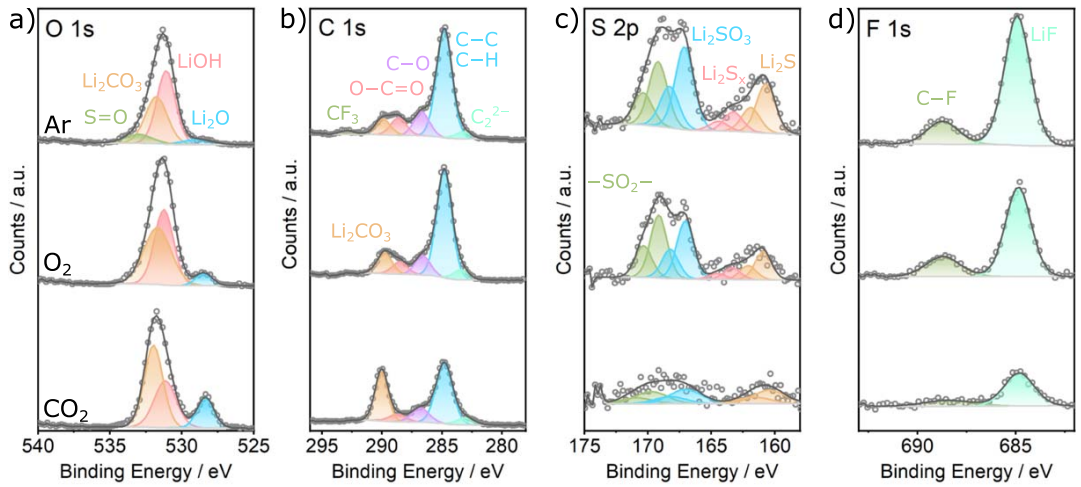

Figure 4. (a) O 1s, (b) C 1s, (c) S 2p and (d) F 1s XP spectra of Li plated on Cu in Ar (top), O_2 (middle) and CO_2 atmosphere (bottom).

with results from Wang et al. and Qiu et al. but conflicts with Lee et al. and Tong et al.[22,23,25,26] Additionally, small amounts of S=O and CF_3 fragments can be seen in O 1s and C 1s spectra of the Ar samples. On the samples from CO_2 atmosphere, however, almost no S 2p or F 1s are present. Hence, $TFSI^-$ degradation can be significantly reduced by cycling under O_2 atmosphere and even more in CO_2 atmosphere.

In context to our SEM and cycling results it becomes evident, that poor cycling performance correlates with the degradation of LiTFSI, even though a F-rich SEI is usually considered as beneficial for the protection of the Li electrode in literature.[26,35,36]

From the Li 1s, O 1s and C 1s spectra, it can be seen that the fraction of Li_2O and Li_2CO_3 in the samples from O_2 and especially CO_2 atmosphere is increased compared to Ar atmosphere. Since these cells also show a significantly higher CE, this indicates that these SEI components have a positive influence on the stability of the Li electrode. In contrast to the findings of Wang et al. and Qiu et al., who assigned the improved cycling performance in O_2 atmosphere to an increased amount of LiOH in the SEI, we could not find a significantly different LiOH content in Ar and O_2 samples.[23,22] Therefore, we rather attribute the improved cycling performance to Li_2O and/or Li_2CO_3.

It has to be noted, that a direct reaction between O_2 and Li can only explain the increased Li_2O content in the SEI, but not the increase in Li_2CO_3. Therefore, we suppose that also the side reaction between O_2 and solvent and subsequent reaction of products from ether oxidation (e.g. CO_2)[13] with the Li electrode play an important role for the improved protection of the Li electrode in the electrolyte with dissolved O_2. This is also supported by the fact that dissolved CO_2 has qualitatively the same influence on the SEI as O_2, only more pronounced.

Influence of native passivation layer.—When comparing reports on the effect of dissolved O_2 on the SEI, we noticed that some groups plated Li on Cu foil[21–23] while others used commercial Li foil[25,26] for plating/stripping experiments. Interestingly, groups who plated Li on Cu observed an improvement of CE and reduction of LiTFSI degradation by introducing O_2 to the cell; groups using Li foil came to opposite results. It is known, that a native passivation layer (NPL) forms on Li foil that is stored in gloveboxes, even when the H_2O and O_2 levels are very low.[37–39] This NPL consists of a Li_2O containing bottom layer and an upper layer comprising LiOH and Li_2CO_3.[32] It is possible that the NPL reacts in a different way than pure Li. Therefore, we also investigated the surface of commercial Li foil (Honjo Metal) in contact to electrolyte with and without O_2 (Fig. 5).

From the XP spectra it is evident, that the amount of $TFSI^-$ fragments is significantly higher on the commercial Li foil, compared to the Li plated on Cu (S=O in O 1s, CF_3 in C 1s as well as S 2p and F 1s in general). Only the Li_2S peak is smaller on the Li foil. This shows that the reactivity of the Li surface changes significantly due to the NPL: More $TFSI^-$ seems to react on the NPL in general. However, the XP spectra also show that the $TFSI^-$ is not completely reduced by the NPL, instead larger fragments remain on the surface (e.g. CF_3, $–SO_2–$). The Li metal surface without NPL, on the other hand, is significantly more reductive, as evidenced by a larger fraction of highly reduced species such as C_2^{2-}, Li_2O and Li_2S.

However, since significantly more $TFSI^-$ reacts with the NPL, the interphase appears to be less stable and passivating than on the freshly deposited Li. This is in line with previous reports that compared cycling of Li metal electrodes with and without NPL. Various techniques (roll pressing, slicing, abrasive blasting) were used to remove the NPL, resulting in decreased interfacial resistance and overpotential and improved cycling performance and reproducibility.[39–41] In order to successfully cycle a Li metal electrode, this should be taken into account during cell manufacture.

Journal of The Electrochemical Society, 2022 **169** 110527

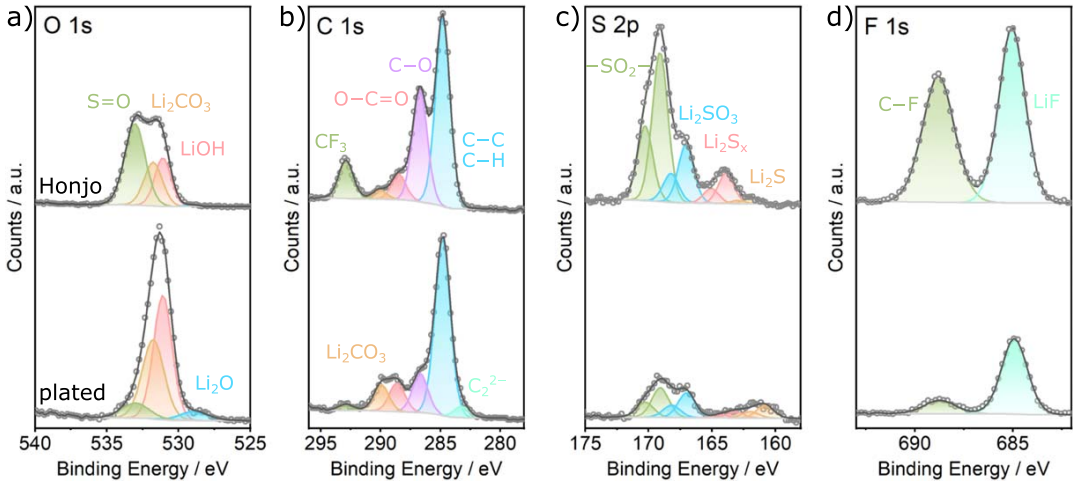

Figure 5. (a) O 1s, (b) C 1s, (c) S 2p and (d) F 1s XP spectra of Honjo Li foil after contact to electrolyte for three days (top) and Li plated on Cu with 0.1 mA cm^{-2} for three days (bottom); both from Ar atmosphere.

Interestingly, we found that the amount of F on the SEI of the commercial Li foil increases when O_2 is dissolved in the electrolyte, hence the opposite trend than on the plated Li (Fig. 6). This matches with the results of Lee et al. and Tong et al.[25,26] and might explain the differences in literature on the influence of dissolved O_2 on Li electrode stability. Since the increase in F content with dissolved O_2 is only observed on the commercial lithium foil and not on the deposited Li, reactions between O_2 and solvent or conducting salt do not seem to be the reason for the differences. We therefore assume that the NPL is first oxidized by the dissolved O_2 and is then more susceptible to side reactions with LiTFSI.

Furthermore, the trend during sputtering is different, too: On the plated Li, the amount of F increases with sputter depth as it is expected since inorganic SEI components such as LiF are usually closer to the Li. On the commercial Li foil, however, the F content decreases during sputtering. This also supports our hypothesis that the NPL reacts with LiTFSI.

This does not necessarily mean that with O_2 also more Li metal reacts. In general, in ex situ experiments with passivated Li foil, only the reactivity of the NPL is probed. From these measurements it is not possible to evaluate the impact of O_2 on the Li underneath the NPL.

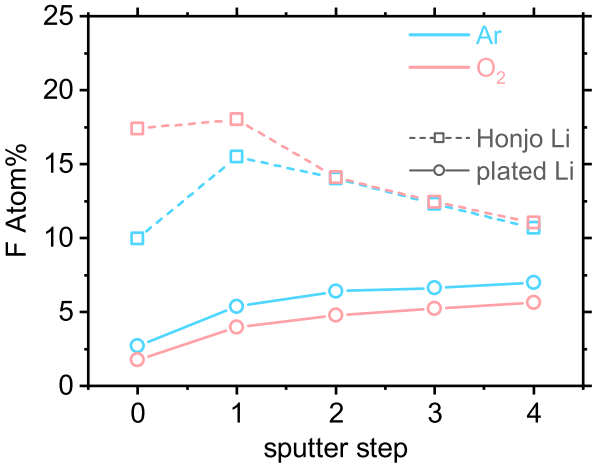

Figure 6. F content calculated from XP spectra of Honjo Li foil after contact to electrolyte for three days (dashed) and Li plated on Cu with 0.1 mA cm^{-2} for three days (solid) in Ar (blue) and O_2 (red) atmosphere.

Conclusion and Outlook

Overall, our work confirms that dissolved O_2 has a positive effect on the stability of the Li metal electrode, regardless of the electrolyte used. We show in plating/stripping experiments on Cu that the CE can be significantly increased by dissolved O_2. We attribute this to the fact that less degradation of the conducting salt (e.g. LiTFSI) takes place with O_2. The SEI therefore contains less F and S, but more Li_2O and Li_2CO_3, which leads to better protection of the Li metal electrode against further side reactions that would lead to Li loss. Dissolved CO_2 has qualitatively the same effect, but changes SEI composition and CE more strongly. In both cases, carrying out the initial plating step in the respective gas atmosphere already improves the CE significantly, even if the subsequent cycling is performed under Ar atmosphere. Such a formation step could also be applied for LMB and should be considered there.

In addition, we could show that the NPL formed on Li foil during its storage changes the SEI and leads to more degradation of the electrolyte. The reactivity of the NPL differs significantly from Li deposited on Cu. In particular, the influence of O_2 is exactly opposite and leads to an increased degradation of the conducting salt on the NPL. This shows that it is very important to use Li that is not passivated when analyzing the SEI. Furthermore, it also offers an explanation for the fact that in some papers a poor influence of dissolved O_2 and increased side reactions are observed.[24–26]

Experimental

Chemicals.—Dimethyl sulfoxide (DMSO), diethylene glycol dimethy ether (diglyme), tetraethylene glycol dimethy ether (tetraglyme), lithium trifluormethanesulfonate (LiOTf) and lithium bis(trifluoromethanesulfonyl)imide (LiTFSI) were purchased from Sigma Aldrich. Lithium bis(fluorosulfonyl)imide (LiFSI), lithium bis(pentafluoroethanesulfonyl)imide (LiBETI), lithium bis(nonafluorobutanesulfonyl)imide (LiNFSI) and lithium nonafluorobutanesulfonate (LiONf) were purchased from TCI Chemicals. All solvents were dried over molecular sieves and the water content was confirmed to be below 10 ppm by Karl-Fischer titration. The conducting salts were dried for 24 h at 60 °C (respectively 80 °C for LiTFSI and LiOTf) under vacuum.

Plating/stripping experiments.—For all electrochemical measurements, a modified Swagelok design ("Giessen cell") was used.[42] The Li metal electrodes were prepared from Li foil (>99.9 wt% Li, Honjo Metal) with a diameter of 12 mm; the Cu electrodes were prepared from Cu foil with a diameter of 12 mm. Two Whatman

Journal of The Electrochemical Society, 2022 **169** 110527

glass fiber separators with a diameter of 12 mm soaked with 70 μL of electrolyte were used as barrier between the electrodes. The concentration of the conducting salt was 1 M in each case. For the electrodes used for further characterization, an additional Celgard separator was placed between electrode and Whatman separator in order to facilitate removal of the separators prior to SEM or XPS measurements.

Cell assembly was carried out in an argon filled glove box (MBraun) with O_2 and H_2O content below 1 ppm. For the cells with dissolved O_2 or CO_2, the gas reservoir of the Swagelok cell was flushed with the respective gas prior to cycling.

Galvanostatic plating/stripping was carried out at a current density of 0.1 mA cm^{-2} referred to the geometrical area of the Li metal electrodes with cutoff voltages of 2.0 V using a Maccor 4300 battery cycler.

Surface characterization.—The Swagelok cells were disassembled in an Ar filled glove box after cycling or resting. Afterwards, the electrodes were rinsed three times with each 100 mL of pure solvent and were then dried in vacuum at room temperature for 12 h.

SEM and EDX.—SEM measurements were performed with a Merlin high resolution electron microscope (Carl Zeiss AG) with an electron acceleration voltage of 3 kV and a probing current of 100 pA. The transfer from the glove box to the SEM was carried out with an Ar filled Leica EM VCT500 shuttle (Leica Microsystems).

XPS.—All samples were transferred using an air-tight, Ar filled transfer module. XPS measurements were carried out with a PHI5000 Versaprobe II system (Physical Electronics Inc.). A monochromatic Al K_α X-ray source (1486.6 eV) with a power of 100 W, a beam voltage of 15 kV and a beam diameter of 200 μm was used. For the survey spectra, a pass energy of 93.9 eV was used; all other spectra were measured with a pass energy of 23.5 eV. All samples were attached to the sample holder with an electrically isolation double-sided tape. Depth profiling was carried out with Ar^+ ions with an acceleration voltage of 1 kV for 1 min per sputter step. For data analysis, CasaXPS 2.3.22 (Casa Software Ltd.) was used. The spectra were calibrated in relation to the signal of adventitious carbon at 284.8 eV. Signal fitting was done with a Shirley background and GL(30) line shapes.

Gas solubility.—O_2 solubilities were determined by gas uptake measurements as described in previous work from our group.[29,43,44] A glass flask (ca. 13 mL) with 2 mL of electrolyte was connected to a ball valve (Swagelok) with a KF flange. The ball valve, was then connected to a stainless stell cross fitting (Swagelok). Additionally, a PAA-33X-V-1 pressure sensor (KELLER AG für Druckmesstechnik), O_2 supply and a vacuum pump were also connected to the cross fitting. Prior to the measurement the solvent was degassed in vacuum. Then a defined amount of O_2 was supplied to the glass flask and the electrolyte was stirred until the pressure was constant. Henry's law solubility constants were then calculated from the pressure decay during stirring. For all electrolytes at least three different measurements at six pressures each were conducted.

Acknowledgments

Financial support by the DFG via the GRK (Research Training Group) 2204 "Substitute Materials for sustainable Energy Technologies" is gratefully acknowledged.

ORCID

Jürgen Janek https://orcid.org/0000-0002-9221-4756

References

1. D. Linden (ed.), *Handbook of Batteries* (McGraw-Hill, New York, NY) 3 ed. (2002).
2. K. M. Abraham and Z. Jiang, *J. Electrochem. Soc.*, **143**, 1 (1996).
3. A. C. Luntz and B. D. McCloskey, *Chem. Rev.*, **114**, 11721 (2014).
4. X.-B. Cheng, R. Zhang, C.-Z. Zhao, and Q. Zhang, *Chem. Rev.*, **117**, 10403 (2017).
5. Z. Peng, S. A. Freunberger, L. J. Hardwick, Y. Chen, V. Giordani, F. Bardé, P. Novák, D. Graham, J.-M. Tarascon, and P. G. Bruce, *Angew. Chem. Int. Ed.*, **50**, 6351 (2011).
6. V. S. Bryantsev, V. Giordani, W. Walker, M. Blanco, S. Zecevic, K. Sasaki, J. Uddin, D. Addison, and G. V. Chase, *J. Phys. Chem. A*, **115**, 12399 (2011).
7. A. Schürmann, B. Luerßen, D. Mollenhauer, J. Janek, and D. Schröder, *Chem. Rev.*, **121**, 12445 (2021).
8. J. Wandt, P. Jakes, J. Granwehr, H. A. Gasteiger, and R.-A. Eichel, *Angew. Chem.*, **128**, 7006 (2016).
9. N. Mahne, S. E. Renfrew, B. D. McCloskey, and S. A. Freunberger, *Angew. Chem. Int. Ed.*, **57**, 5529 (2018).
10. E. Mourad et al., *Energy Environ. Sci.*, **12**, 2559 (2019).
11. B. D. McCloskey, A. Speidel, R. Scheffler, D. C. Miller, V. Viswanathan, J. S. Hummelshøj, J. K. Nørskov, and A. C. Luntz, *J. Phys. Chem. Lett.*, **3**, 997 (2012).
12. M. M. Ottakam Thotiyl, S. A. Freunberger, Z. Peng, and P. G. Bruce, *J. Am. Chem. Soc.*, **135**, 494 (2013).
13. S. A. Freunberger, Y. Chen, N. E. Drewett, L. J. Hardwick, F. Bardé, and P. G. Bruce, *Angew. Chem. Int. Ed.*, **50**, 8609 (2011).
14. M. Balaish, A. Kraytsberg, and Y. Ein-Eli, *Phys. Chem. Chemy. Phys.*, **16**, 2801 (2014).
15. E. Nasybulin, W. Xu, M. H. Engelhard, Z. Nie, S. D. Burton, L. Cosimbescu, M. E. Gross, and J.-G. Zhang, *J. Phys. Chem. C*, **117**, 2635 (2013).
16. G. M. Veith, J. Nanda, L. H. Delmau, and N. J. Dudney, *J. Phys. Chem. Lett.*, **3**, 1242 (2012).
17. X. Bi, K. Amine, and J. Lu, *J. Mater. Chem. A*, **8**, 3563 (2020).
18. W. Zhang, Y. Huang, Y. Liu, L. Wang, S. Chou, and H. Liu, *Adv. Energy Mater.*, **9**, 1900464 (2019).
19. Y.-S. Hong, C.-Z. Zhao, Y. Xiao, R. Xu, J.-J. Xu, J.-Q. Huang, Q. Zhang, X. Yu, and H. Li, *Batter. Supercaps*, **2**, 638 (2019).
20. X. Yao, Q. Dong, Q. Cheng, and D. Wang, *Angew. Chem. Int. Ed.*, **55**, 11344 (2016).
21. M. Roberts, R. Younesi, W. Richardson, J. Liu, T. Gustafsson, J. Zhu, and K. Edström, *ECS Electrochem. Lett.*, **3**, A62 (2014).
22. F. Qiu, X. Zhang, Y. Qiao, X. Zhang, H. Deng, T. Shi, P. He, and H. Zhou, *Energy Storage Mater.*, **12**, 176 (2018).
23. E. Wang, S. Dey, T. Liu, S. Menkin, and C. P. Grey, *ACS Energy Lett.*, **5**, 1088 (2020).
24. R. S. Assary, J. Lu, P. Du, X. Luo, X. Zhang, Y. Ren, L. A Curtiss, and K Amine, *ChemSusChem*, **6**, 51 (2013).
25. H. Lee, D. J. Lee, J. N. Lee, J. Song, Y. Lee, M. H. Ryou, J. K. Park, and Y. M. Lee, *Electrochimica Acta*, **123**, 419 (2014).
26. B. Tong, J. Huang, Z. Zhou, and Z. Peng, *Adv. Mater.*, **30**, 1704841 (2018).
27. F. Qiu, S. Ren, X. Mu, Y. Liu, X. Zhang, P. He, and H. Zhou, *Energy Storage Mater.*, **26**, 443 (2020).
28. S. Nanda, A. Gupta, and A. Manthiram, *Adv. Energy Mater.*, **11**, 2000804 (2021).
29. R. Haas, M. Murat, M. Weiss, J. Janek, A. Natan, and D. Schröder, *J. Electrochem. Soc.*, **168**, 070504 (2021).
30. M. Saito, T. Fujinami, S. Yamada, T. Ishikawa, H. Otsuka, K. Ito, and Y. Kubo, *J. Electrochem. Soc.*, **164**, A2872 (2017).
31. K. N. Wood and G. Teeter, *ACS Appl. Energy Mater.*, **1**, 4493 (2018).
32. S.-K. Otto, Y. Moryson, T. Krauskopf, K. Peppler, J. Sann, J. Janek, and A. Henss, *Chem. Mater.*, **33**, 859 (2021).
33. B. S. Parimalam and B. L. Lucht, *J. Electrochem. Soc.*, **165**, A251 (2018).
34. D. Aurbach, I. Weissman, A. Schechter, and H. Cohen, *Langmuir*, **12**, 3991 (1996).
35. N. Xu, J. Shi, G. Liu, X. Yang, J. Zheng, Z. Zhang, and Y. Yang, *J. Power Sources Adv.*, **7**, 100043 (2021).
36. N. Aspern, G.-V. Röschenthaler, M. Winter, and I. Cekic-Laskovic, *Angew. Chem. Int. Ed.*, **58**, 15978 (2019).
37. S.-K. Otto, T. Fuchs, Y. Moryson, C. Lerch, B. Mogwitz, J. Sann, J. Janek, and A. Henss, *ACS Appl. Energy Mater.*, **4**, 12798 (2021).
38. S. Bessette, P. Hovington, H. Demers, M. Golozar, P. Bouchard, R. Gauvin, and K. Zaghib, *Microsc. Microanal.*, **25**, 866 (2019).
39. J. Becking, A. Gröbmeyer, M. Kolek, U. Rodehorst, S. Schulze, M. Winter, P. Bieker, and M. C. Stan, *Adv. Mater. Interfaces*, **4**, 1700166 (2017).
40. H. Wang, Z.-L. Yi, F.-Y. Su, G. Song, L.-J. Xie, Z.-B. Wang, and C.-M. Chen, *Journal of Power Sources*, **520**, 230817 (2022).
41. A. Wolf, H. Lorrmann, A. Flegler, A. J. Wolf, A. Guerfi, K. Mandel, and G. A. Giffin, *Energy Technology*, **9**, 2100455 (2021).
42. C. L. Bender, P. Hartmann, M. Vračar, P. Adelhelm, and J. Janek, *Adv. Energy Mater.*, **4**, 1301863 (2014).
43. A. Schürmann, R. Haas, M. Murat, N. Kuritz, M. Balaish, Y. Ein-Eli, J. Janek, A. Natan, and D. Schröder, *J. Electrochem. Soc.*, **165**, A3095 (2018).
44. P. Hartmann, D. Grübl, H. Sommer, J. Janek, W. G. Bessler, and P. Adelhelm, *J. Phys. Chem. C*, **118**, 1461 (2014).

4 Conclusions & Outlook

In this work, the influence of dissolved O_2 on the lithium electrode was systematically investigated and the results were published in two publications. Initially, the solubility and diffusivity of O_2 (and other gases) in different electrolytes was investigated in the first publication *"Understanding the Transport of Atmospheric Gases in Liquid Electrolytes for Lithium–Air Batteries"*. The second publication *"The Influence of Oxygen Dissolved in the Liquid Electrolyte on Lithium Metal Anodes"* then compared lithium plating and stripping in O_2-containing and O_2-free electrolytes and focused on differences in SEI composition and CE.

In the first publication, the solubilities of O_2, N_2 and CO_2 were investigated by gas uptake measurements. It was found that for O_2 and N_2 there is a linear relationship between $\ln L$ and σ in pure solvents. In the future these findings can help to estimate the solubility of O_2 in other solvents from the surface tension, which is often known, without the need for additional experiments. Even if the surface tension is not known, it can be determined experimentally or simulated with less effort.[87] Furthermore, the effect of conducting salts on gas solubility was investigated. Remarkably, an increase in O_2 solubility was observed for DMSO through the addition of LiTFSI, i.e. a so-called salting-in effect. The CO_2 solubility however decreases, which means that the ratio of CO_2 to O_2 solubility in the electrolyte depends on the type and concentration of the conducting salt and can thus be modified. In later experiments with larger conducting salts such as LiNFSI, the O_2 solubility was further increased in both DMSO- and diglyme-based electrolytes. It is often assumed that the solubility of other components decreases when a conducting salt is added due to the salting-out effect. The fact that this is not always the case shows that the selection of the conducting salt offers a hitherto underestimated possibility of specifically modifying the O_2 solubility in the electrolyte. These results can also be transferred to other electrolytes and thus be relevant for other metal–O_2 batteries as well. All in all, valuable findings were obtained that will make it possible in the future to predict the O_2 solubility in new electrolytes or to develop tailored electrolytes with optimized gas solubility. In addition, the diffusion coefficients of the same gases in electrolytes and solvents were determined both experimentally and calculated in MD simulations. A good qualitative agreement between experiment and simulation was found. In the future, this may allow the partial elimination of experiments, which can be replaced by simulations. Since a comparatively large amount of solvent/electrolyte is needed for the experimental determination of diffusion coefficients by gas uptake measurements, costs as well as environmental impact and working time can be reduced. Overall, the results obtained in this publication can help in the development of tailored electrolytes for Li–O_2 batteries. The limiting current density that can be achieved in the battery can be calculated directly from the parameters H^{cp} and D determined therein. Although other factors are also relevant for electrolyte development, it is particularly important that the solubility and diffusion of O_2 are as high as possible in batteries where fast charging

and discharging is required. Additionally, the values measured here can be used by researchers who work on simulations and models of processes in Li–O_2 batteries.

In the second publication, it was shown that O_2 and CO_2 have a positive influence on the stability of the lithium electrode. In a comparison of plating/stripping experiments, the CE was significantly higher when the electrolyte was saturated with the respective gas. In addition, it could be shown that the SEI in the O_2 and CO_2 containing electrolytes contained significantly less products of the TFSI degradation. Both gases therefore have a positive influence on the formation of the SEI. Compared with organic SEI-forming additives, they have the additional advantage that they are very simple molecules and do not require complex synthesis. It is also interesting to note that a significant improvement in CE in multiple plating/stripping cycles was also observed, when only the initial plating was carried out in the respective gas atmosphere and the subsequent cycling took place in the O_2- and CO_2-free electrolytes. In general, dissolved gases seems to be a promising approach to alter the SEI on the lithium electrode and improve the CE. Therefore, also other gases should be tested in future experiments. In order to gain a better understanding of the processes taking place in the battery, gases such as CO or C_2H_4, which emerge from electrolyte degradation, are probably of particular interest in this context. The fact that the CE in electrolytes containing CO_2 was still significantly better than in electrolytes containing only O_2 shows that CO_2 contamination from the ambient air in Li–air batteries is not a problem, at least for the lithium electrode. Even at the cathode, small amounts of dissolved CO_2 do not seem to affect the performance of the battery, hence a CO_2 content of 0.1% in the air does not seem to be a problem for battery operation.[88] Even in Li–O_2 batteries with a gas reservoir, one can therefore consider using a minimal amount of CO_2 to increase the stability of the lithium electrode. However, it has to be noted that also in this publication it could not be conclusively clarified whether the dissolved O_2 reacts directly with the lithium electrode or whether the electrolyte degradation triggered by O_2 plays the decisive role in the formation of the SEI. To clarify this, further research in the field is necessary. Additionally, we have demonstrated that the NPL on commercial lithium foil also alters the SEI and causes greater deterioration of the electrolyte, especially the conducting salt. The reactivity of the NPL differs significantly from that of lithium plated on copper, with O_2 having an opposite effect, resulting in even more increased degradation of the conducting salt on the NPL. This underscores the importance of using fresh lithium when studying the SEI. Moreover it offers an explanation for the observed negative impact of dissolved O_2 and increased side reactions that were observed in some studies.[13,14,89]

Given that LIBs are making rapid progress and practical energy density continues to increase, it is unclear whether a Li–O_2 battery can achieve significant improvement in this regard. It is also questionable whether the Li–O_2 battery can ever be developed to the point where commercialization is possible. Nevertheless, research on Li–O_2 batteries should be pursued further. On the one hand, there is still a chance to solve the existing problems. Even if the Li–O_2 battery will probably not be able to completely replace LIBs, there will be various application areas with special requirements where the Li–O_2 battery can be beneficial. The demand for batteries is still high and a decline is not expected in the near future. On the other hand, many findings from research on Li–O_2 batteries can be transferred to other battery systems and thus contribute to their progress. This also applies to the results of this thesis. The results obtained on solubility and diffusion of O_2 are also applicable to other metal O_2 batteries (Na, Al, Zn, Mg). Since the understanding of O_2 solubility has been significantly improved in this thesis, it is also possible to

estimate the solubility in electrolytes used in other metal O_2 batteries. The results from the second publication, on the other hand, may also prove useful for LMBs, since both O_2 and CO_2 have a positive effect on lithium electrode stability and can be used to aid SEI formation. Also in LMBs, O_2 may be present in the electrolyte if it is formed by oxidation of the cathode materials. However, since LMBs mainly use carbonate-based electrolytes, which are less stable to reactive oxygen species, only CO_2 is probably relevant for this battery type. Anyway, further experiments are needed to clarify whether the improvements in CE with dissolved CO_2 observed in ether and DMSO-based electrolytes are also present in carbonate-based electrolytes. In addition, longer plating stripping experiments with more cycles are necessary, as well as cycling in full cells. The fact that freshly plated lithium behaves differently than lithium foil with NPL shows that this should also be taken into account when manufacturing batteries with lithium electrode. Since plated lithium causes less LiTFSI degradation than lithium foils with NPL, the NPL should be removed or anode-free concepts can be applied in the case of LMBs.

Overall, the understanding of the influence of O_2 on the lithium electrode was significantly improved in this thesis. A particularly important point was to consider the results in the context of previous publications, which made it possible to resolve the existing contradictions in the literature. The work on gas solubility has also shown that it can be very valuable to look at older literature in detail and also to search outside the battery community. Furthermore, it is important to consider the results outside the Li–O_2 context, as they may also be relevant for other battery systems. Batteries are a very important part of our energy supply in the future and the demand for them will not decrease in the next years, rather the opposite. Therefore, it is important to continuously improve them, which makes further research necessary, ideally also on Li–O_2 batteries.

Bibliography

[1] T. Hummel, **2023**, *https://www.sueddeutsche.de/politik/klimaziele-deutschland-treibhausgase-emissionen-1.5768935*, accessed: 06.04.2023.

[2] Gesetz für den Ausbau erneuerbarer Energien (Erneuerbare-Energien-Gesetz - EEG 2023), **2014**.

[3] W.-J. Kwak, Rosy, D. Sharon, C. Xia, H. Kim, L. R. Johnson, P. G. Bruce, L. F. Nazar, Y.-K. Sun, A. A. Frimer, M. Noked, S. A. Freunberger, D. Aurbach, *Chem. Rev.* **2020**, *120*, 6626–6683.

[4] M. M. Thackeray, C. Wolverton, E. D. Isaacs, *Energy Environ. Sci.* **2012**, *5*, 7854–7863.

[5] J. Janek, W. G. Zeier, *Nat. Energy* **2016**, *1*, 1–4.

[6] X.-B. Cheng, R. Zhang, C.-Z. Zhao, Q. Zhang, *Chem. Rev.* **2017**, *117*, 10403–10473.

[7] H.-F. Wang, Q. Xu, *Matter* **2019**, *1*, 565–595.

[8] A. C. Luntz, B. D. McCloskey, *Chem. Rev.* **2014**, *114*, 11721–11750.

[9] J. Betz, G. Bieker, P. Meister, T. Placke, M. Winter, R. Schmuch, *Adv. Energy Mater.* **2019**, *9*, 1803170.

[10] T. Liu, J. P. Vivek, E. W. Zhao, J. Lei, N. Garcia-Araez, C. P. Grey, *Chem. Rev.* **2020**, *120*, 6558–6625.

[11] D. Geng, N. Ding, T. S. A. Hor, S. W. Chien, Z. Liu, D. Wuu, X. Sun, Y. Zong, *Adv. Energy Mater.* **2016**, *6*, 1502164.

[12] D. Aurbach, *J. Electrochem. Soc.* **1989**, *136*, 906.

[13] R. S. Assary, J. Lu, P. Du, X. Luo, X. Zhang, Y. Ren, L. A. Curtiss, K. Amine, *ChemSusChem* **2013**, *6*, 51–55.

[14] H. Lee, D. J. Lee, J. N. Lee, J. Song, Y. Lee, M. H. Ryou, J. K. Park, Y. M. Lee, *Electrochim. Acta* **2014**, *123*, 419–425.

[15] M. Roberts, R. Younesi, W. Richardson, J. Liu, T. Gustafsson, J. Zhu, K. Edström, *ECS Electrochem. Lett.* **2014**, *3*, A62.

[16] F. Qiu, X. Zhang, Y. Qiao, X. Zhang, H. Deng, T. Shi, P. He, H. Zhou, *Energy Stor. Mater.* **2018**, *12*, 176–182.

[17] E. Wang, S. Dey, T. Liu, S. Menkin, C. P. Grey, *ACS Energy Lett.* **2020**, *5*, 1088–1094.

[18] K. M. Abraham, Z. Jiang, *J. Electrochem. Soc.* **1996**, *143*, 1.

[19] X. Bi, K. Amine, J. Lu, *J. Mater. Chem. A* **2020**, *8*, 3563–3573.

[20] M. Balaish, A. Kraytsberg, Y. Ein-Eli, *Phys. Chem. Chem. Phys.* **2014**, *16*, 2801–2822.

[21] Y. Li, X. Wang, S. Dong, X. Chen, G. Cui, *Adv. Energy Mater.* **2016**, *6*, 1600751.

[22] W. Xu, J. Xiao, J. Zhang, D. Wang, J.-G. Zhang, *J. Electrochem. Soc.* **2009**, *156*, A773.

[23] S. R. Gowda, A. Brunet, G. M. Wallraff, B. D. McCloskey, *J. Phys. Chem. Lett.* **2013**, *4*, 276–279.

[24] J. Zhang, W. Xu, W. Liu, *J. Power Sources* **2010**, *195*, 7438–7444.

[25] Z. Peng, S. A. Freunberger, L. J. Hardwick, Y. Chen, V. Giordani, F. Bardé, P. Novák, D. Graham, J.-M. Tarascon, P. G. Bruce, *Angew. Chem. Int. Ed.* **2011**, *50*, 6351–6355.

[26] L. Johnson, C. Li, Z. Liu, Y. Chen, S. A. Freunberger, P. C. Ashok, B. B. Praveen, K. Dholakia, J.-M. Tarascon, P. G. Bruce, *Nat. Chem.* **2014**, *6*, 1091–1099.

[27] N. B. Aetukuri, B. D. McCloskey, J. M. García, L. E. Krupp, V. Viswanathan, A. C. Luntz, *Nat. Chem.* **2015**, *7*, 50–56.

[28] L. D. Griffith, A. E. Sleightholme, J. F. Mansfield, D. J. Siegel, C. W. Monroe, *ACS Appl. Mater. Interfaces* **2015**, *7*, 7670–7678.

[29] B. D. Adams, C. Radtke, R. Black, M. L. Trudeau, K. Zaghib, L. F. Nazar, *Energy Environ. Sci.* **2013**, *6*, 1772–1778.

[30] K. Chen, D.-Y. Yang, G. Huang, X.-B. Zhang, *Acc. Chem. Res.* **2021**, *54*, 632–641.

[31] X. Yao, Q. Dong, Q. Cheng, D. Wang, *Angew. Chem. Int. Ed.* **2016**, *55*, 11344–11353.

[32] X.-B. Cheng, R. Zhang, C.-Z. Zhao, F. Wei, J.-G. Zhang, Q. Zhang, *Adv. Sci.* **2016**, *3*, 1500213.

[33] G. Bieker, M. Winter, P. Bieker, *Phys. Chem. Chem. Phys.* **2015**, *17*, 8670–8679.

[34] S. H. Park, Y. J. Cheon, Y. J. Lee, K. H. Shin, Y. Y. Hwang, Y. S. Jeong, Y. J. Lee, *ACS Appl. Mater. Interfaces* **2019**, *11*, 30872–30879.

[35] V. Viswanathan, K. S. Thygesen, J. S. Hummelshøj, J. K. Nørskov, G. Girishkumar, B. D. McCloskey, A. C. Luntz, *J. Chem. Phys.* **2011**, *135*, 214704.

[36] M. M. Ottakam Thotiyl, S. A. Freunberger, Z. Peng, P. G. Bruce, *J. Am. Chem. Soc.* **2013**, *135*, 494–500.

[37] B. D. McCloskey, A. Speidel, R. Scheffler, D. C. Miller, V. Viswanathan, J. S. Hummelshøj, J. K. Nørskov, A. C. Luntz, *J. Phys. Chem. Lett.* **2012**, *3*, 997–1001.

[38] A. Schürmann, B. Luerßen, D. Mollenhauer, J. Janek, D. Schröder, *Chem. Rev.* **2021**, *121*, 12445–12464.

[39] N. Mahne, S. E. Renfrew, B. D. McCloskey, S. A. Freunberger, *Angew. Chem. Int. Ed.* **2018**, *57*, 5529–5533.

[40] N. Mahne, B. Schafzahl, C. Leypold, M. Leypold, S. Grumm, A. Leitgeb, G. A. Strohmeier, M. Wilkening, O. Fontaine, D. Kramer, C. Slugovc, S. M. Borisov, S. A. Freunberger, *Nat. Energy* **2017**, *2*, 1–9.

[41] S. A. Freunberger, Y. Chen, N. E. Drewett, L. J. Hardwick, F. Bardé, P. G. Bruce, *Angew. Chem. Int. Ed.* **2011**, *50*, 8609–8613.

[42] V. S. Bryantsev, J. Uddin, V. Giordani, W. Walker, D. Addison, G. V. Chase, *J. Electrochem. Soc.* **2012**, *160*, A160.

[43] D. G. Kwabi, T. P. Batcho, C. V. Amanchukwu, N. Ortiz-Vitoriano, P. Hammond, C. V. Thompson, Y. Shao-Horn, *J. Phys. Chem. Lett.* **2014**, *5*, 2850–2856.

[44] B. D. McCloskey, D. S. Bethune, R. M. Shelby, T. Mori, R. Scheffler, A. Speidel, M. Sherwood, A. C. Luntz, *J. Phys. Chem. Lett.* **2012**, *3*, 3043–3047.

[45] C. O. Laoire, S. Mukerjee, K. M. Abraham, E. J. Plichta, M. A. Hendrickson, *J. Phys. Chem. C* **2010**, *114*, 9178–9186.

[46] S. A. Freunberger, Y. Chen, Z. Peng, J. M. Griffin, L. J. Hardwick, F. Bardé, P. Novák, P. G. Bruce, *J. Am. Chem. Soc.* **2011**, *133*, 8040–8047.

[47] V. S. Bryantsev, M. Blanco, *J. Phys. Chem. Lett.* **2011**, *2*, 379–383.

[48] E. Nasybulin, W. Xu, M. H. Engelhard, Z. Nie, S. D. Burton, L. Cosimbescu, M. E. Gross, J.-G. Zhang, *J. Phys. Chem. C* **2013**, *117*, 2635–2645.

[49] Y. Yamada, K. Furukawa, K. Sodeyama, K. Kikuchi, M. Yaegashi, Y. Tateyama, A. Yamada, *J. Am. Chem. Soc.* **2014**, *136*, 5039–5046.

[50] L. Wang, K. Uosaki, H. Noguchi, *J. Phys. Chem. C* **2020**, *124*, 12381–12389.

[51] B. Liu, W. Xu, P. Yan, S. T. Kim, M. H. Engelhard, X. Sun, D. Mei, J. Cho, C.-M. Wang, J.-G. Zhang, *Adv. Energy Mater.* **2017**, *7*, 1602605.

[52] J. Heine, P. Hilbig, X. Qi, P. Niehoff, M. Winter, P. Bieker, *J. Electrochem. Soc.* **2015**, *162*, A1094.

[53] J. Guo, Z. Wen, M. Wu, J. Jin, Y. Liu, *Electrochem. Commun.* **2015**, *51*, 59–63.

[54] Y. K. Petit, C. Leypold, N. Mahne, E. Mourad, L. Schafzahl, C. Slugovc, S. M. Borisov, S. A. Freunberger, *Angew. Chem. Int. Ed.* **2019**, *58*, 6535–6539.

[55] B. J. Bergner, A. Schürmann, K. Peppler, A. Garsuch, J. Janek, *J. Am. Chem. Soc.* **2014**, *136*, 15054–15064.

[56] Y. Chen, S. A. Freunberger, Z. Peng, O. Fontaine, P. G. Bruce, *Nat. Chem.* **2013**, *5*, 489–494.

[57] J.-B. Park, S. H. Lee, H.-G. Jung, D. Aurbach, Y.-K. Sun, *Adv. Mater.* **2018**, *30*, 1704162.

[58] W.-J. Kwak, H. Kim, Y. K. Petit, C. Leypold, T. T. Nguyen, N. Mahne, P. Redfern, L. A. Curtiss, H.-G. Jung, S. M. Borisov, S. A. Freunberger, Y.-K. Sun, *Nat. Commun.* **2019**, *10*, 1380.

[59] W.-J. Kwak, S. A. Freunberger, H. Kim, J. Park, T. T. Nguyen, H.-G. Jung, H. R. Byon, Y.-K. Sun, *ACS Catal.* **2019**, *9*, 9914–9922.

[60] W.-J. Kwak, J. Park, H. Kim, J. M. Joo, D. Aurbach, H. R. Byon, Y.-K. Sun, *ACS Energy Lett.* **2020**, *5*, 2122–2129.

[61] B. J. Bergner, M. R. Busche, R. Pinedo, B. B. Berkes, D. Schröder, J. Janek, *ACS Appl. Mater. Interfaces* **2016**, *8*, 7756–7765.

[62] X. Gao, Y. Chen, L. Johnson, P. G. Bruce, *Nat. Mater.* **2016**, *15*, 882–888.

[63] S. S. Zhang, J. Read, *J. Power Sources* **2011**, *196*, 2867–2870.

[64] Y. Wang, D. Zheng, X.-Q. Yang, D. Qu, *Energy Environ. Sci.* **2011**, *4*, 3697–3702.

[65] H. Wan, Q. Bai, Z. Peng, Y. Mao, Z. Liu, H. He, D. Wang, J. Xie, G. Wu, *J. Mater. Chem. A* **2017**, *5*, 24617–24620.

[66] R. Battino, H. L. Clever, *Chem. Rev.* **1966**, *66*, 395–463.

[67] J. H. Hildebrand, R. Scott, **1950**, 75–92.

[68] H. H. Uhlig, *J. Phys. Chem.* **1937**, *41*, 1215–1226.

[69] R. Haas, M. Murat, M. Weiss, J. Janek, A. Natan, D. Schröder, *J. Electrochem. Soc.* **2021**, *168*, 070504.

[70] M. Balaish, A. Kraytsberg, Y. Ein-Eli, *ChemElectroChem* **2014**, *1*, 90–94.

[71] A. Schürmann, R. Haas, M. Murat, N. Kuritz, M. Balaish, Y. Ein-Eli, J. Janek, A. Natan, D. Schröder, *J. Electrochem. Soc.* **2018**, *165*, A3095.

[72] F. A. Long, W. F. McDevit, *Chem. Rev.* **1952**, *51*, 119–169.

[73] J. O. Bockris, J. Bowler-Reed, J. A. Kitchener, *Trans. Faraday Soc.* **1951**, *47*, 184–192.

[74] P. Debye, *Z. Phys. Chem.* **1927**, *130*, 56–64.

[75] J. Lindberg, B. Endródi, G. Åvall, P. Johansson, A. Cornell, G. Lindbergh, *J. Phys. Chem. C* **2018**, *122*, 1913–1920.

[76] R. Haas, J. Janek, *J. Electrochem. Soc.* **2022**, *169*, 110527.

[77] X.-h. Yang, Y.-y. Xia, *J. Solid State Electrochem.* **2009**, *14*, 109.

[78] H. Wang, X. Wang, M. Li, L. Zheng, D. Guan, X. Huang, J. Xu, J. Yu, *Adv. Mater.* **2020**, *32*, 2002559.

[79] M. Marinaro, P. Balasubramanian, E. Gucciardi, S. Theil, L. Jörissen, M. Wohlfahrt-Mehrens, *ChemSusChem* **2015**, *8*, 3139–3145.

[80] S. H. Lee, J.-B. Park, H.-S. Lim, Y.-K. Sun, *Adv. Energy Mater.* **2017**, *7*, 1602417.

[81] D. J. Lee, H. Lee, Y.-J. Kim, J.-K. Park, H.-T. Kim, *Adv. Mater.* **2016**, *28*, 857–863.

[82] B. J. Bergner, C. Hofmann, A. Schürmann, D. Schröder, K. Peppler, P. R. Schreiner, J. Janek, *Phys. Chem. Chem. Phys.* **2015**, *17*, 31769–31779.

[83] R. Younesi, M. Hahlin, M. Roberts, K. Edström, *J. Power Sources* **2013**, *225*, 40–45.

[84] D. Aurbach, Y. Gofer, J. Langzam, *J. Electrochem. Soc.* **1989**, *136*, 3198.

[85] M. Saito, T. Fujinami, S. Yamada, T. Ishikawa, H. Otsuka, K. Ito, Y. Kubo, *J. Electrochem. Soc.* **2017**, *164*, A2872–A2880.

[86] B. Tong, J. Huang, Z. Zhou, Z. Peng, *Adv. Mater.* **2018**, *30*, 1704841.

[87] V. Goussard, F. Duprat, V. Gerbaud, J. L. Ploix, G. Dreyfus, V. Nardello-Rataj, J. M. Aubry, *J. Chem. Inf. Model.* **2017**, *57*, 2986–2995.

[88] T. Wang, X. Pan, J. Chen, Y. Chen, *J. Phys. Chem. Lett.* **2021**, *12*, 4799–4804.

[89] J. Tong, S. Wu, N. von Solms, X. Liang, F. Huo, Q. Zhou, H. He, S. Zhang, *Frontiers in Chemistry* **2020**, *7*, 1–10.

[90] N. R. Levy, P. Tereshchuk, A. Natan, R. Haas, D. Schröder, J. Janek, P. Jakes, R. A. Eichel, Y. Ein-Eli, *J. Power Sources* **2021**, *514*, 230597.

[91] R. Haas, C. Pompe, M. Osenberg, A. Hilger, I. Manke, B. Mogwitz, U. Maitra, D. Langsdorf, D. Schröder, *Energy Technol.* **2019**, *7*, 1801146.

[92] L. Medenbach, C. L. Bender, R. Haas, B. Mogwitz, C. Pompe, P. Adelhelm, D. Schröder, J. Janek, *Energy Technol.* **2017**, *5*, 2265–2274.

A Supporting Informations

A.1 Supporting Information on Publication 1

Supporting Information

Understanding the Transport of Atmospheric Gases in Liquid Electrolytes for Lithium–Air Batteries

Author Names: Ronja Haas[1,2], Michael Murat[3,4], Manuel Weiss[1,2], Jürgen Janek[1,2], Amir Natan[3,5,z], Daniel Schröder[6,z]

Affiliations:

[1] Institute of Physical Chemistry, Justus Liebig University Giessen, 35392 Giessen, Germany

[2] Center for Materials Research (LaMa), Justus Liebig University Giessen, 35392 Giessen, Germany

[3] Department of Physical Electronics, Tel Aviv University, Tel Aviv 69978, Israel

[4] Soreq NRC, Yavne 81800, Israel

[5] The Raymond and Beverly Sackler Center for Computational Molecular and Materials Science, Tel Aviv University, Tel Aviv 69978, Israel

[6] Institute of Energy and Process Systems Engineering (InES), Technische Universität Braunschweig, 38106 Braunschweig, Germany

[z] d.schroeder@tu-braunschweig.de, amirnatan@post.tau.ac.il

Table S1: Surface tension at 25 °C given in mN m^{-1}. [a]measured in this work, [b]taken from reference,[1] [c]taken from reference.[2]

solvent	surface tension / mN m^{-1}
diglyme	29.4[a]
triglyme	31.8[a]
tetraglyme	33.5[a]
DMSO	42.9[b]
perfluorooctane	14.5[c]
perfluorononane	15.4[c]
perfluorodecalin	19.4[c]

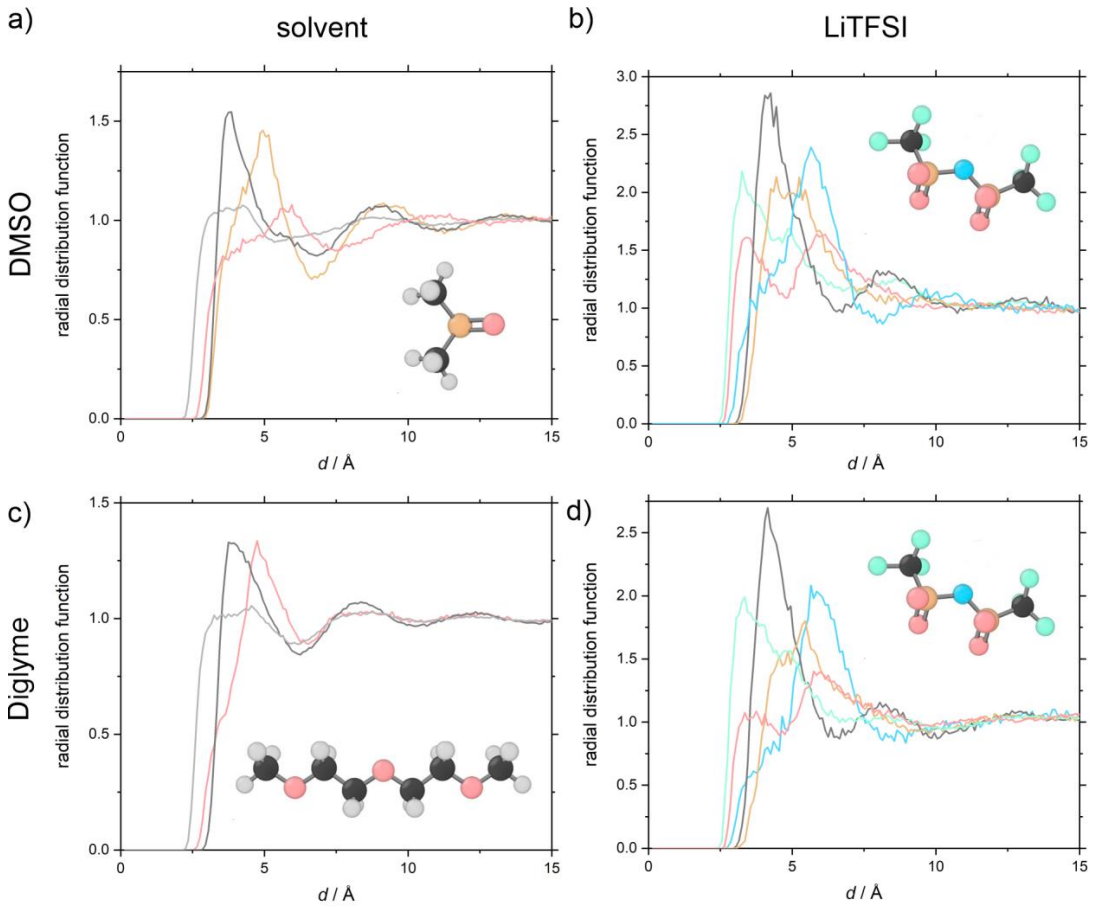

Figure S1: Radial distribution functions of O_2 in 1 M LiTFSI solutions in (a) and (b) DMSO and (c) and (d) diglyme. The distance of O_2 to different atoms of (a) and (c) the solvent and (b) and (d) the TFSI anion is displayed. The colors are chosen according to the images of the molecules: O red, C black, H gray, S yellow, N blue and F green.

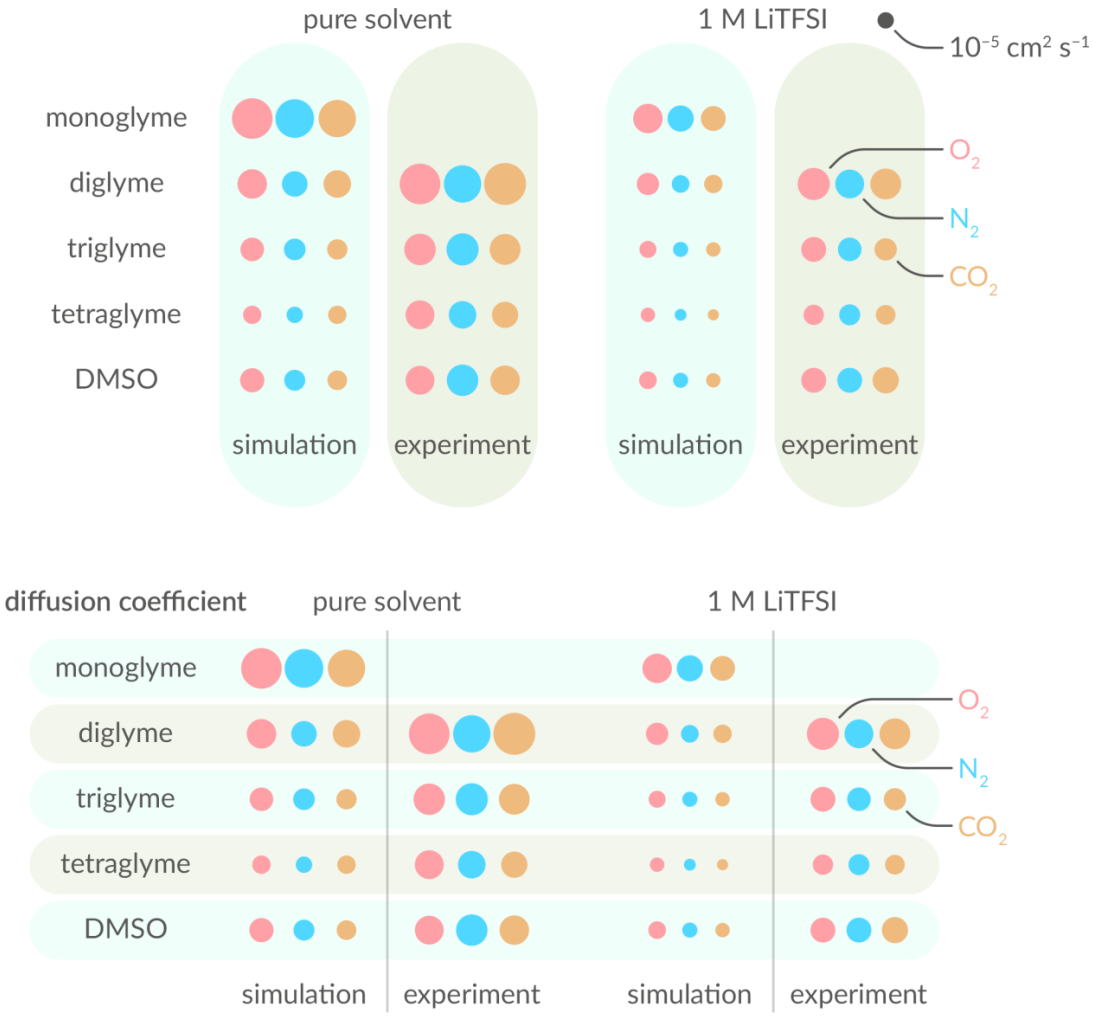

Figure S2: Graphical representation of the different diffusion coefficients in the pure solvents and the solvents with 1 M of LiTFSI. The diffusion coefficient is represented by the area of the circles. O_2 is shown with red, N_2 is shown with blue and CO_2 is shown with orange. *D* is decreasing with the chain length of glyme ethers and lower in the solution with 1 M LiTFSI compared to the pure solvents.

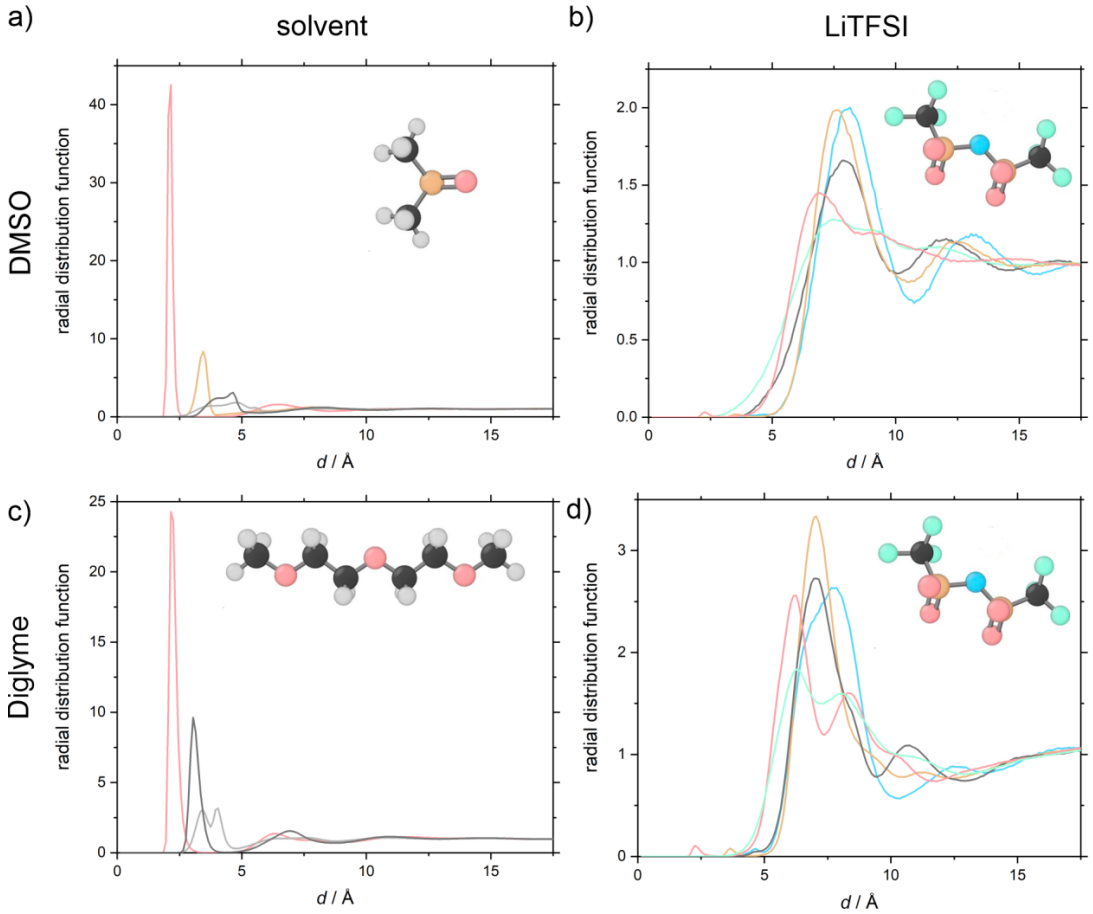

Figure S3: Radial distribution functions of Li^+ in 1 M LiTFSI solutions in (a) and (b) DMSO and (c) and (d) diglyme. The distance of Li^+ to different atoms of (a) and (c) the solvent and (b) and (d) the TFSI anion is displayed. The colors are chosen according to the images of the molecules: O red, C black, H gray, S yellow, N blue and F green.

References

1. J. J. Jasper, *J. Phys. Chem. Ref. Data*, **1**, 841–1010 (1972).
2. M. G. Freire, P. J. Carvalho, A. J. Queimada, I. M. Marrucho, and J. A. P. Coutinho, *J. Chem. Eng. Data*, **51**, 1820–1824 (2006).

A.2 Supporting Information on Publication 2

The Influence of Oxygen Dissolved in the Liquid Electrolyte on Lithium Metal Anodes

Ronja Haas[1,2], *Jürgen Janek*[1,2,*]

[1]Institute of Physical Chemistry, Justus-Liebig University Giessen, 35392 Giessen, Germany
[2]Center for Materials Research (LaMa), Justus-Liebig University Giessen, 35392 Giessen, Germany
*Email: juergen.janek@phys.chemie.uni-giessen.de

1 Cycling performance with dissolved CO_2

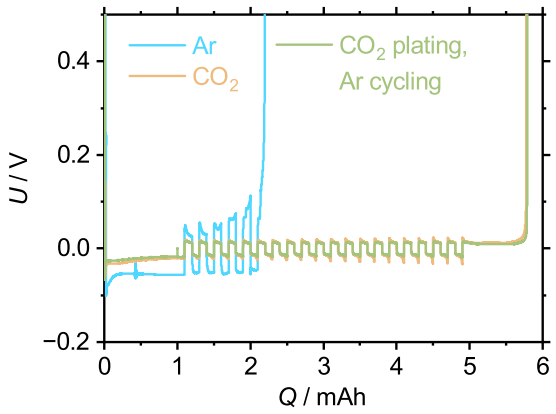

Figure 1: Plating/stripping experiments with only initial plating in CO_2 atmosphere compared to cycling with constant gas pressure.

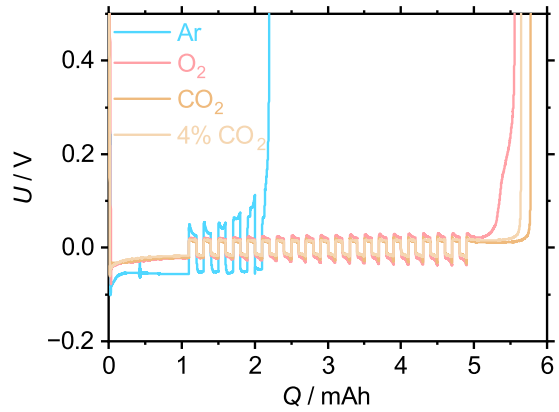

Figure 2: Plating/stripping experiment with 40 mbar CO_2 partial pressure compared to 1 bar pressure of CO_2, O_2 and Ar.

2 O_2 solubility in different electrolytes

Table 1: Henry's law solubility constant (H^{cp}) of O_2 in different electrolytes given in $\mathrm{mmol\,L^{-1}\,bar^{-1}}$. Average of at least three different measurements. [a]Taken from[1]

Solvent	Salt	$H^{cp}(O_2)$
DMSO	1 M LiTFSI	2.7[a]
Tetraglyme	1 M LiTFSI	4.1[a]
Diglyme	1 M LiOTf	5.6
Diglyme	1 M LiONf	5.4
Diglyme	1 M LiFSI	5.3
Diglyme	1 M LiTFSI	5.9[a]
Diglyme	1 M LiBETI	6.8
Diglyme	1 M LiNFSI	7.6

3 Assignment of XPS peaks

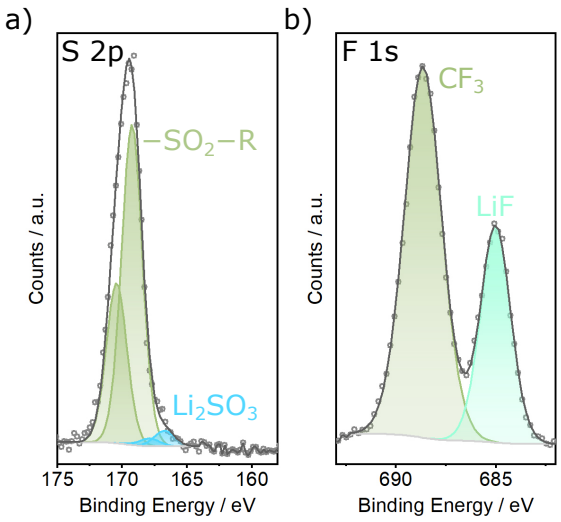

Figure 3: XP spectra of pure LiTFSI pulver. Small amounts of LiF and Li_2SO_3 form due to X-ray or sputter damage. However, the fraction of these species is much lower than on the Li electrodes. Therefore, LiTFSI degradation is not caused by X-ray or sputter damage, but mainly by side reactions during plating/stripping.

Table 2: Assignment of XPS peaks. [a]Taken from spectra of pure LiTFSI powder.

Line	Compound	Position	Reference
Li 1s	LiOH	54.9 eV	[2,3]
	Li_2CO_3	55.5 eV	[2,3]
	Li_2O	53.8 eV	[2,3]
O 1s	LiOH	531.1 eV	[2,3]
	Li_2CO_3	531.8 eV	[2,3]
	Li_2O	528.4 eV	[2,3]
	S=O	533.0 eV	[a]
C 1s	CF_3	292.9 eV	[a]
	Li_2CO_3	289.9 eV	[3,4]
	O−C=O	288.6 eV	
	C−O	286.7 eV	
	C−C, C−H	284.8 eV	used for calibration
	C_2^{2-}	283.3 eV	[4]
S 2p	$-SO_2-R$	169.1 eV	[a]
	Li_2SO_3	167.1 eV	[5,6]
	S^0 from Li_2S_x	163.4 eV	[5,6]
	Li_2S_2	160.9 eV	[5,6]
F 1s	C−F	688.7 eV	[a]
	LiF	684.9 eV	[5,6]

References

[1] R. Haas, M. Murat, M. Weiss, J. Janek, A. Natan, D. Schröder, *J. Electrochem. Soc.* **2021**, *168*, 070504.

[2] S.-K. Otto, Y. Moryson, T. Krauskopf, K. Peppler, J. Sann, J. Janek, A. Henss, *Chem. Mater.* **2021**, *33*, 859–867.

[3] K. N. Wood, G. Teeter, *ACS Appl. Energy Mater.* **2018**, *1*, 4493–4504.

[4] K. Kanamura, S. Shiraishi, H. Tamura, Z.-i. Takehara, *J. Electrochem. Soc.* **1994**, *141*, 2379.

[5] M. I. Nandasiri, L. E. Camacho-Forero, A. M. Schwarz, V. Shutthanandan, S. Thevuthasan, P. B. Balbuena, K. T. Mueller, V. Murugesan, *Chem. Mater.* **2017**, *29*, 4728–4737.

[6] V. Shutthanandan, M. Nandasiri, J. Zheng, M. H. Engelhard, W. Xu, S. Thevuthasan, V. Murugesan, *J. Electron Spectrosc. Relat. Phenom.* **2019**, *231*, 2–10.

B Abbreviations and Symbols

B.1 List of Abbreviations

CE	Coulomb efficiency
CIP	contact ion pair
DABCOnium	1-pentyl-1,4-diazabicyclo[2.2.2]octan-1-ium
DEMS	differential electrochemical mass spectrometry
diglyme, 2G	diethylene glycol dimethyl ether
DMSO	dimethyl sulfoxide
DN	donor number
EIS	electrochemical impedance spectroscopy
FEC	fluoroethylene carbonate
FT-IR	Fourier transform infrared spectroscopy
IL	ionic liquid
LIB	lithium ion battery
LiBETI	lithium bis(pentafluoroethanesulfonyl)imide
LiBOB	lithium bis(oxalato)borate
LiFSI	lithium bis(fluorosulfonyl)imide
LiNFSI	lithium bis(nonafluorobutanesulfonyl)imide
LiOTf	lithium trifluoromethanesulfonate
LiTFSI	lithium bis(trifluoromethanesulfonyl)imide
LiTNFSI	lithium (trifluoromethanesulfonyl)(n-nonafluorobutanesulfonyl)imide
LMB	lithium metal battery
MD	molecular dynamics
MeCN	acentonitrile
NPL	native passivation layer
OER	oxygen evolution reaction
ORR	oxygen reduction reaction
PC	propylene carbonate
PFC	perfluorocarbons
RM	redox mediator
SEI	solid-electrolyte interphase
SEM	scanning electron microscopy
SSIP	shared solvent ion pair
tetraglyme, 4G	tetraethylene glycol dimethyl ether
THF	tetrahydrofurane
triglyme, 3G	triethylene glycol dimethyl ether
VC	vinylene carbonate
XPS	x-ray photoelectron spectroscopy
XRD	x-ray diffraction

B.2 List of Symbols

A	surface area of an electrode
b	co-volume of a real gas
c	concentration
$c_{\text{gas}}^{\text{atm}}$	concentration of gas in the atmosphere
$c_{\text{gas}}^{\text{sol}}$	concentration of gas in the liquid
D	diffusion coefficient
E	interaction energy of a gas solute with a solvent
F	Faraday constant
H^{cp}	Henry's law solubility constant
I_{lim}	mass-transport limiting current
j	Flux
k_{B}	Boltzmann constant
L	Ostwald coefficient
n	number of transferred electrons
p	pressure
Q	capacity
r	radius
R	ideal gas constant
t	time
T	temperature
U	voltage
V_{gas}	volume of gas
V_{sol}	volume of solvent
x	distance
δ	thickness of the Nernst layer
η	dynamic viscosity
μ	mobility
σ	surface tension

C Scientific Contributions

C.1 List of Publications

- **R. Haas**, J. Janek; The Influence of Oxyen Dissolved in the Liquid Electrolyte on Lithium Metal Anodes, *J. Electrochem. Soc.*, **2022**, *169*, 110527. [76]
- N. R. Levy, P. Tereshchuk, A. Natan, **R. Haas**, D. Schröder, J. Janek, P. Jakes, R. A. Eichel, Y. Ein-Eli; Hybridization of carbon nanotube tissue and MnO_2 as a generic advanced air cathode in metal–air batteries, *J. Power Sources*, **2021**, *514*, 230597. [90]
- **R. Haas**, M. Murat, M. Weiss, J. Janek, A. Natan, D. Schröder; Understanding the Transport of Atmospheric Gases in Liquid ELectrolytes for Lithium–Air Batteries, *J. Electrochem. Soc.*, **2021**, *168*, 070504. [69]
- **R. Haas**, C. Pompe, M. Osenberg, A. Hilger, I. Manke, B. Mogwitz, U. Maitra, D. Langsdorf, D. Schröder; Practical Implications of Using a Solid Electrolyte in Batteries aith a Sodium Anode: A Combined X-Ray Tomogrphy and Model-Based Study, *Energy Technol.*, **2019**, *7*, 1801146. [91]
- A. Schürmann, **R. Haas**, M. Murat, N. Kuritz, M. Balaish, Y. Ein-Eli, J. Janek, A. Natan, D. Schröder; Diffusivity and Solbility of Oxygen in Solvents for Metal/Oxygen Batteries: A Combined Theoretical and Experimental Study, *J. Electrochem. Soc.*, **2018**, *165*, A3095–A3099. [71]
- L. Medenbach, C. L. Bender, **R. Haas**, B. Mogwitz, C. Pompe, P. Adelhelm, D. Schröder, J. Janek; Origins of Dendrite Formation in Sodium–Oxygen Batteries and Possible Counter Measures, *Energy Technol.*, **2017**, *5*, 2265–2274. [92]

C.2 List of Conference Contributions

- **R. Haas**, M. Murat, J. Janek, A. Natan, D. Schröder; Elucidating the Solubility and Diffusivity of Atmospheric Gases in a Wide Variation of Liquid Electrolytes for Lithium–Air Batteries, *239th ECS Meeting (online)*, **June 2021**, Oral presentation.
- **R. Haas**, J. Janek; Influence of Dissolved O_2 on SEI Formation and Lithium Electrode Stability, *IMLB Sydney*, **June 2022**, Poster presentation.

D Acknowledgements

Finally, I would like to thank all those who have contributed to the successful completion of this work.

First of all, I would like to thank my supervisor Prof. Dr. Jürgen Janek for the opportunity to work in his research group. I would also like to thank him for his constant support during the work on my doctoral thesis.

Furthermore, I would like to thank Prof. Dr. Daniel Schröder for his support and supervision since my third semester and for beeing the second reviewer of this thesis.

Additionally, I would like to thank Luca Kaufer, who has supported me in experimental work since his bachelor thesis in various study projects and as student assistant.

I would also like to thank the entire working group and especially my office colleagues Julian, Laura, Christoph and Manuel for the good working atmosphere.

Finally, I would like to thank my family and friends for their support. My special thanks go to Jo, Stella and Marielle.